Distributed Observers-based Cooperative Platooning Tracking Control and Intermittent Optimization for Connected Automated Vehicles with Unknown Jerk Dynamics

Bohui Wang, *Senior Member, IEEE,* **Rong Su,** *Senior Member, IEEE,* **Yun Lu,** *Member, IEEE,* **Lingyin Huang,** *Member, IEEE,*
Nanbin Zhao, Zhijian Hu [*]

September 1, 2022

[*]B. Wang, R. Su, Y. Lu, L. Huang, N. Zhao and Z. Hu are with the School of Electrical and Electronic Engineering, Nanyang Technological University, Singapore 639798 (e-mail: bhwang@ntu.edu.sg; rsu@ntu.edu.sg; yun.lu@ntu.edu.sg; lingying.huang@ntu.edu.sg; nanbin001@e.ntu.edu.sg; zhijian.hu@ntu.edu.sg).

ABSTRACT

The unknown sharp changes of vehicle acceleration rates, also called the unknown jerk dynamics, may significantly affect the driving performance of the leader vehicle in a platoon, resulting in more drastic car-following movements in platooning tracking control, which could cause safety and traffic capacity concerns. To address these issues, in this paper, we investigate cooperative platooning tracking control and intermittent optimization problems for connected automated vehicles (CAVs) with a nonlinear car-following model. We assume that the external inputs of the leader CAV contain unknown but bounded jerk parameters, and the acceleration signals of the leader CAV are known only to a few neighboring follower CAVs in a free-design but directed communication network. To solve these problems, a distributed observer law is developed to provide a reference signal expressed as an estimated unknown jerk dynamic of the leader CAV and implemented by each follower CAV. Then, a novel distributed platooning tracking control protocol is proposed to construct the cooperative tracking controllers under identical inter-vehicle constraints, which can ensure a desired safety distance among the CAVs and allow each follower CAV to track their leader CAV by using only local information interaction. We also present a novel intermittent sampling condition and a robust intermittent optimization design that can ensure optimally scheduled feedback gains for the cooperative platooning tracking controllers to minimize the control cost under nonidentical inter-vehicle constraints and unknown jerk dynamics. Simulation case studies are carried out to illustrate the effectiveness of the proposed approaches

Index Terms—**Connected automated vehicles (CAVs); cooperative platooning control; intermittent optimization; distributed observers; car-following model; unknown dynamics; formation control.**

I. Introduction

AS one key part of smart city, intelligent transportation systems have attracted a lot of attention by virtue of the advanced management and monitoring systems with smart sensors and excellent information transformation based on Vehicle-to-X (or V2X) technology [1]–[3]. Such emerging techniques provide new means to reduce traffic congestion, fuel consumption, and environmental footprints and enhance safety. To optimize the energy consumption of autonomous vehicles, a framework that integrates optimal control and coordination for connected automated vehicles(CAVs) at urban traffic intersections was studied in [4], where a continuous flow of CAVs crossing two adjacent intersections was considered. Subsequently, a decentralized control strategy,

aiming for smart junction crossing with minimum fuel consumption in a traffic lightless network, was proposed in [5]. Notably, coordination and interaction of CAVs are challenging issues due to the complex vehicle dynamics and unpredictable traffic conditions. Considering that unknown traffic disturbances, such as the sudden appearance of pedestrians, may significantly affect the dynamics of the CAVs, a safety distance among the moving CAVs must be ensured in real-time. However, as pointed out in [6], maintaining a small gap among the CAVs may require aggressive throttling and braking, and may lead to suboptimal operation of the powertrain when the velocity profile is variable. Specifically, unknown jerk dynamics make the situation even worse, leading to more challenging cooperative platooning tracking control and optimization problems of CAVs. Therefore, this paper attempts to solve these problems by developing a cooperative platooning tracking strategy and distributed observer techniques, motivated by the recent developments in the consensus community [7]–[10].

One key objective of platooning tracking control for the CAVs is to develop different vehicle longitudinal control algorithms by using limited inter-vehicle interaction information. One typical strategy is Adaptive Cruise Control (ACC), which automatically adapts the velocity of a vehicle to ensure a desired distance to the preceding vehicle. However, ACC also amplifies disturbances in upstream directions at small-time gaps [11], [12], causing, e.g., string instability [13]. Cooperative Adaptive Cruise Control (CACC) is an enhancement of ACC enabled by V2V communication, which employs wireless vehicle-to-vehicle communication and onboard measurements to achieve smaller inter-vehicle distances [14]–[16]. However, it is noted that ACC and CACC assume an ideal control topology, where the design of the controller is based on a static and fixed communication pattern [17], [18]. If the communication pattern is different from the designed one, for example, due to network impairments or a change of platooning control strategy, the performance of ACC and CACC may degrade, and even become unable to safely control the platoon. In response to the aforementioned insufficiency, the consensus has been proposed as an effective tool to design control algorithms able to handle space constraints [19]–[22]. In this spirit, the vehicular fleet was modeled in [23] as a second-order linear system that communicates over a wireless network with arbitrary topology (instead of those introduced in the classical CACC [24]). Besides, [6] treats the traffic cooperative control problem as a distributed formation tracking control problem using the multi-agent consensus schemes, which was also addressed in [25]–[28] to maintain a specified queue form (e.g., constant space distance).

Notice that ACC or CACC only assists vehicle driving, instead of taking it over. Thus, specific car-following models are needed, when applying ACC or CACC. A car-following model describes how one driver follows immediately the preceding cars. In this framework, the following behaviors of individual vehicles and the perception mechanism of drivers are two important factors in describing traffic models. For example, an optimal velocity model was introduced in [29], to describe the characteristics of real traffic flow, such as traffic jams or stop-and-go traffic waves. A new car-following model incorporating the effects of the lateral gap and roadside device communication was proposed in [30], to capture the characteristics of electric vehicle traffic streams in

transportation-cyber-physical systems. A general framework for the car-following model has been proposed in [31] which aims to facilitate the easier implementation of stability analysis in traffic flow. Although these studies are very helpful in achieving the cooperative platooning tracking control of CAVs, the dynamics of the leader CAV are usually assumed to be either a constant speed or a known acceleration profile, which is hard to be implemented in the actual traffic network owing to the complex traffic conditions and the unpredictable driving behaviors.

This paper addresses the cooperative platooning tracking control and intermittent optimization problems for the CAVs with a specific car-following model and unknown jerk dynamics by developing a distributed observer protocol under a free-design but directed communication topology, where the leader CAV will be affected by the unknown traffic network conditions, e.g., stop-and-go, or sudden acceleration caused by unpredicted traffic congestion. We first formulate a distributed cooperative platooning tracking control framework for CAVs whose protocol relies on a novel distributed observer of the unknown jerk dynamics of the leader CAV that utilizes only the neighboring information under a free-design but directed communication network. Different from the existing works [17], [25], [26], [28], [32]–[35], some realistic inter-vehicle constraints and unknown jerk signals are explicitly considered in the current framework, which may not be easily handled in those mentioned existing works. To achieve this result, we need to assume the boundedness of the unknown jerk signals. When compared with the existing ACC [11], [12] and CACC [14], [15] strategies that assume a static control topology, which means that the design of the controller is based on a fixed communication paradigm [17], [18], we can solve the problem of cooperative platooning tracking control for CAVs based on a reconfigurable (not fixed) controller at design-time to match the network and the platoon characteristics. We secondly present a novel car-following model, which, in contrast to the existing analysis frameworks that mainly involve linear dynamics [15], [17], [28], [35], takes the nonlinear modeling of drivers' perception mechanism and unknown jerk dynamics into account to provide an optimal velocity model for each CAV. Unlike the assumption imposed in string stability that the perturbation strictly attenuates for each leader-follower pair as it propagates away from the first leader [13], [36], the driver in this new car-following model can easily recover from small disturbances in real traffic and return to a steady car-following model state over time by exploring the cooperative perception. We finally present a novel feedback gain scheduling approach by developing a robust intermittent optimization algorithm, which is different from the previous works [25]–[28] that require a fixed feedback gain, and permits a design of optimal feedback gains intermittently, making our cooperative tracking control strategy different from existing works and more powerful for the vehicle control.

The paper is organized as follows: Section II introduces the problem formulation and necessary preliminaries. Section III provides the main results on the design of cooperative platooning tracking control for the platoon CAVs with a nonlinear car-following model under a directed communication topology. Section IV presents an intermittent optimization design to calculate the optimal feedback gains of the cooperative platooning tracking controller. Section V illustrates the effectiveness of the proposed

approaches with simulations and conclusions are drawn in Section VI.

II. Preliminaries and problem formulation

A. Notations

The following notations are introduced throughout this paper: $M \geq 0$ ($M \leq 0$) means that the matrix M is positive semi-definite (negative semi-definite). The sets of nonnegative integers and real numbers are denoted by $\mathbb{N}$ and $\mathbb{R}$, respectively. Let 0 be a zero vector with an appropriate dimension, which is clear from the context. Similar notations are adopted for $\mathbf{1}$ and I for one vector and identity matrix. For a vector $x = [x_1, x_2, \ldots, x_p]^\top$, let $||x||_q = (\sum_{i=1}^{p} |x_i|^q)^{\frac{1}{q}}$ with $q > 0$ being the q-normal. $\mathbf{sgn}(x) = [\mathbf{sgn}(x_1), \mathbf{sgn}(x_2), \ldots, \mathbf{sgn}(x_p)]^\top$ and $(\mathbf{sgn}(x))^{\frac{1}{2}} = [|x_1|^{\frac{1}{2}}\mathbf{sgn}(x_1), |x_2|^{\frac{1}{2}}\mathbf{sgn}(x_2), \ldots, |x_p|^{\frac{1}{2}}\mathbf{sgn}(x_p)]^\top$, where $\mathbf{sgn}(\cdot)$ is the signum function. The Kronecker product, denoted by $\otimes$, facilitates the manipulation of matrices by the following properties: (1) $(A \otimes B)(C \otimes D) = AC \otimes BD$; (2) $(A \otimes B)^\top = A^\top \otimes B^\top$; (3) $A \otimes (B + C) = A \otimes B + A \otimes C$; and (4) $(A \otimes B)^{-1} = A^{-1} \otimes B^{-1}$, for any given invertible matrices A and B.

B. Preliminaries

We hereby recall the graph theory to describe the connected links among the CAVs [10], [28], [37]. A communication topology consisting of $(N + 1)$ CAVs can be defined as a directed graph $G = (\mathcal{V}, \mathcal{E}, A)$, where $\mathcal{V} = \{v_1, \cdots, v_{N+1}\}$ denotes the vehicles in the group, the edge set $\mathcal{E} \in \mathcal{V} \times \mathcal{V}$ denotes the neighboring relations among the vehicles, and the adjacency matrix is $A = [a_{ij}]_{N+1 \times N+1}$ with non-negative elements a_{ij}. A directed path generated from v_i to v_j is a finite ordered sequence of edges $(v_i, v_{k_1}), \cdots, (v_{k_g}, v_j)$, with distinct nodes $v_{k_{m_0}}$, $m_0 = 1, \cdots, \hbar$. Define the Laplacian matrix $L = [l_{ij}]_{N+1 \times N+1}$ of graph $\mathcal{G}$ satisfying $l_{ij} = -a_{ij}$, $i \neq j$; otherwise $\sum_{k=1, k \neq i}^{N+1} a_{ik}$, $i = j$. A fixed directed graph G is said to contain a directed spanning tree if there exists a node that can reach any other node via a directed path. Without loss of generality, the following definition and lemmas are introduced.

Lemma 1: [37] For a fixed directed graph $\mathcal{G}$, the Laplacian matrix L of $\mathcal{G}$ has a simple zero eigenvalue and all the other eigenvalues have positive real parts if and only if the graph $\mathcal{G}$ contains a directed spanning tree.

Definition 1: [28], [37] A square matrix $A = [a_{ij}]$ is a non-singular M-matrix, if all the leading principal minors of A are positive and satisfy $a_{ij} \leq 0$ for all $i \neq j$.

Lemma 2: [28], [37] There exists a matrix $A = [a_{ij}] \in \mathbb{R}^{n \times n}$ satisfying $a_{ij} \leq 0$ for any $i \neq j$. Then, we have the following equivalent statements: i) A is a nonsingular M-matrix; ii) All eigenvalues of A have positive real parts; and iii) There exists a positive definite matrix $\Theta \in \mathbb{R}^{n \times n}$ such that $A^\top \Theta + \Theta A > 0$.

Lemma 3: [38] Given a symmetric matrix $S = \begin{bmatrix} s_{11} & s_{12} \\ s_{12}^\top & s_{22} \end{bmatrix}$, the following conditions are equivalent: *i)* $S < 0$; *ii)* $s_{11} < 0$, $s_{22} - s_{12}^\top s_{11}^{-1} S_{12} < 0$; *iii* $s_{22} < 0$, $s_{11} - s_{12} s^{-1} s_{22} s_{12}^\top < 0$.

Lemma 4: [39] Let $Q \in \mathbb{R}^{N \times N}$ be a symmetric matrix and $W \in \mathbb{R}^{n \times n}$ be a symmetric positive semi-definite matrix. Then, for any $x \in \mathbb{R}^{nN}$, the inequality $\lambda_{\min}(Q) x^\top (I_N \otimes W) x \le x^\top (Q \otimes W) x \le \lambda_{\max}(Q) x^\top (I_N \otimes W) x$ holds, where $\lambda_{\min}(Q)$, $\lambda_{\max}(Q)$ are the minimal and maximum eigenvalues of Q.

C. Problem formulation

This paper considers the cooperative platooning tracking control and intermittent optimization problem for CAVs, cruising in a specified traffic-signal-free lane with continuous-time second-order integral dynamics. Suppose that there are N follower CAVs and one leader CAV. Let $\mathcal{F} = \{1, \cdots, N\}$ be the set of the follower CAVs, where the dynamics of the follower i are described as follows:

$$
\begin{aligned}
\dot{s}_i(t) &= v_i(t), \\
\dot{v}_i(t) &= a_i(t), i \in \mathcal{F},
\end{aligned}
\tag{1}
$$

where $s_i(t) \in \mathbb{R}$, $v_i(t) \in \mathbb{R}$, $a_i(t) \in \mathbb{R}$ are the position, velocity, and acceleration of the i-th CAV, respectively. The system (1) is widely used for system-level CAV control [32], [33]; see [34] and [40] for more general discrete-time models and more complex heterogeneous multi-agent models with different vehicle parameters, respectively.

We define the label of the leader CAV as 0, whose dynamics are described as follows:

$$
\begin{aligned}
\dot{s}_0(t) &= v_0(t), \\
\dot{v}_0(t) &= a_0(t), \\
\dot{a}_0(t) &= a_0(t) + \rho(t),
\end{aligned}
\tag{2}
$$

where $s_0(t) \in \mathbb{R}$, $v_0(t) \in \mathbb{R}$, $a_0(t) \in \mathbb{R}$ are the position, velocity, and acceleration of the leader CAV respectively. Equation $\dot{a}_0(t) = a_0(t) + \rho(t)$ represents the unknown jerk dynamics of the leader CAV where $\rho(t)$ is an unknown piecewise continuous but bounded external signal, whose upper bound $\bar{\rho}$, i.e., $||\rho(t)|| \le \bar{\rho}$, is known. This setup can capture many acceleration profiles used in the literature and vehicle simulation software [41].

Remark 1: It is noted that the jerk dynamics can be formulated by a piecewise function to describe the different acceleration scenarios for the leader CAV, which does not affect the continuous signals of position, velocity, and acceleration of platoon CAVs because the unknown jerk dynamics of the leader CAV can be regarded as the external factors from the complex traffic environment. For different traffic conditions, the variable driver intentions will show impassable vehicle dynamics. In order to propose an effective vehicle control solution, we here consider a piecewise function to describe common driving behaviors of drivers to actually capture the situations of constant velocity, constant acceleration, or sharp acceleration adjustment. The details design will be described in the simulation case studies of this paper. In general, the jerk dynamics are also used to check the safety requirement [42] and detect safety-critical events [43]. It has been shown that, although a minimum gap maximizes the road through-

put [44]–[46], and possibly reduces the vehicle air drag [47], [48], maintaining a small gap may require aggressive throttling and braking, leading to suboptimal operations of the powertrain when the velocity profile is variable [6]. Thus, unknown jerk dynamics will cause great impacts on platoon performance and vehicle safety. In this paper, we consider the influence of the leader CAV's sudden acceleration on the cooperative platooning tracking control by proposing a specific way of estimating the jerk dynamics to ensure safety and improve traffic capacity.

Remark 2: In fact, the leader in the platoon may be a real or a virtual CAV that aims to provide a reference state that is tracked by the follower CAVs. Specifically, it is easy to verify that whether the platoon behaviors can be solved by our cooperative platooning tracking control protocols (which will be given later) has nothing to do with the labels of the CAVs. For the convenience of analysis, it is assumed that the index 0 represents the leader CAV.

Remark 3: The considered system dynamics of the leader vehicle are very practical, which can cover the general linear system with unknown but bounded inputs, as shown below

$$
\dot{x} = Ax + B\rho
$$

where $A = \begin{bmatrix} 0, 1, 0 \\ 0, 0, 1 \\ 0, 0, 1 \end{bmatrix}$, $B = \begin{bmatrix} 0 \\ 0 \\ 1 \end{bmatrix}$ $x = [s_0, v_0, a_0]^\top$. However, different from the control technologies developed in the consensus theory for linear systems with unknown but bounded inputs as made in [40], we here consider a more realistic system model, in which the leader, affected by the external complex traffic environment, will show an uncertain dynamic adjustment of an unknown jerk, and all the follower vehicles will use the optimal model to perceive such changes and design the efficient cooperative platoon control strategy. There is no relevant research on this issue at present, so our research is novel and challenging. Our goal is to propose a new mechanism to model this process, and to better respond to complex traffic environments with human-like driving behaviors, i.e., emergencies, and improve driving safety and comfort.

To describe how one driver follows immediately the preceding CAVs with their perception information, we further extend a specific car-following model, also called the "optimal velocity model" (OVM), referred to [29], [49], [50]. Based on this, the dynamics of the follower CAV i can be redescribed as follows

$$
\begin{aligned}
\dot{s}_i(t) &= v_i(t), \\
\dot{v}_i(t) &= Y_i(v_i(t)) + u_i(t), \\
u_i(t) &= \zeta_i(t) + \hat{u}_i(t), i \in \mathcal{F},
\end{aligned}
\tag{3}
$$

where $Y_i(v_i(t))$ represents how the CAV i responds to a stimulus from other CAVs which will be designed later, $u_i(t)$ represents the cooperative tracking control input, which can integrate the acceleration estimate $\zeta_i(t)$, $i \in \mathcal{F}$, for the leader CAV 0 and the regulation tracking information $\hat{u}_i(t)$ for the follower CAV i that will be introduced shortly.

To ensure that the velocity and acceleration input of each CAV are within a given admissible range, the following vehicle constraints

are imposed

$$
\begin{aligned}
&v_{\min} \leq v_0(t) \leq v_{\max}, \\
&a_{\min} \leq a_0(t) \leq a_{\max}, \\
&v_{\min} \leq v_i(t) \leq v_{\max}, \\
&a_{\min} \leq \zeta_i(t) \leq a_{\max}, i \in \mathcal{F},
\end{aligned} \tag{4}
$$

where $v_{\min}$ and $v_{\max}$ are the minimum and maximum speed limits, and $a_{\min}$ and $a_{\max}$ are the minimum and maximum acceleration for all the CAVs, respectively. Similar to [34], the acceleration/deceleration bounds for each CAV are assumed to be pre-specified and known. It is noted that as the basic framework, the bounds of the constraints are first considered to be identical according to the recommended speed. The nonidentical case will be considered in the next section.

To analyze the equilibrium dynamics of the platoon system, we would like to introduce a new system variable $\xi_i(t) = [s_i(t), v_i(t)]^\top$, $i = 0, \ldots, N$, and two system weight matrices $T_1 = [1, 0]^\top$ and $T_2 = [0, 1]^\top$. Then, the cooperative tracking dynamics of the CAVs (3) can be rewritten as

$$
\dot{\xi}_i(t) = T_1 T_2^\top \xi_i(t) + T_2 u_i(t) + T_2 Y_i(v_i(t)), i = 0, \ldots, N, \tag{5}
$$

where $u_0(t) = a_0(t)$ and $Y_0(v_0(t)) = 0$ due to the fact that the leader CAV has no incoming information from neighbors.

Furthermore, we define the platoon variable for the follower CAVs as $h = [h_1^\top, \ldots, h_N^\top]^\top$, where $h_i = [h_{is}, h_{iv}]^\top$ is the platoon vector, i.e., desired platoon state (distance and speed) relative to the leader CAV for the follower $i, i \in \mathcal{F}$. By convention, we have $h_{0s} = 0, h_{0v} = 0$. Therefore, the control objective here is to design an effective cooperative platooning tracking control algorithm such that all the follower CAVs asymptotically reach the desired platoon distance with respect to the leader CAV with unknown jerk dynamics, which can be defined as follows:

Definition 2: The CAVs (2) and (3) are said to achieve the co-operative platooning tracking control if the designed cooperative tracking control input $u_i(t)$ with proper feedback gains and local information interaction can guarantee that the states of all the follower CAVs converge to the state of the leader CAV with the desired platoon distance h_{is}, that is

$$
\lim_{t \to \infty} \|\xi_i(t) - h_i - \xi_0(t)\| = 0, \forall i \in \mathcal{F}, \tag{6}
$$

It is clear that the rear-end collision problem will arise if the platoon distance h_{is} is not sufficient for the minimum safe cruising distance d_c. To prevent any rear-end collision, we define the specific safety cruising constraint h_{is} satisfying

$$
\lim_{t \to \infty} \|s_i(t) - s_0(t)\| = h_{is} \geq d_c. \tag{7}
$$

which is a safety cruising constraint for the objective (6).

Remark 4: Notably, the rear-end safety constraints are usually presented in terms of an allowable headway since it assumes that the CAVs travel on the lane with a safety distance from the beginning. In fact, there are two major spacing policies for platoon CAVs: the constant distance policy and the constant time headway policy. The constant distance policy can provide a simple and easy way to implement the platoon formulation and lead to

a very high traffic capacity because the desired distance between two consecutive CAVs is independent of their velocities [51]–[53]. For the constant time headway policy, the desired inter-vehicle range varies with the CAVs' velocities, which accords with driver behaviors to some extent but limits the achievable traffic capacity [54], especially for aging drivers. In fact, even for experienced drivers, it is difficult for them to keep a steady speed under complex road conditions. Especially in the face of sudden accidents or congestion, stop-and-go situations will lead to a frequent adjustment of driving speed, thus leading to frequent switching of desired vehicle spacing, which may further increase the risk of accidents. Therefore, the desired platoon distance h_{is} in this paper is considered as a fixed safe spacing which implies that all the follower CAVs are controlled to move in a rigid formation following a leader CAV to achieve a high traffic capacity and a more smooth car-following environment.

To achieve the control objective (6), this paper proposes the following cooperative platooning tracking control protocols by employing a distributed observer design under a directed communication topology

$$
u_i(t) = \zeta_i(t) + \hat{u}_i(t) , \tag{8}
$$

$$
\hat{u}_i(t) = cK_1 \left(\sum_{j=0}^{N} a_{ij}((s_j(t) - h_{js}) - (s_i(t) - h_{is})) \right) \tag{9}
$$

$$
+ cK_2 \left(\sum_{j=0}^{N} a_{ij}((v_j(t) - h_{jv}) - (v_i(t) - h_{iv})) \right) , \tag{10}
$$

$$
\dot{\zeta}_i(t) = \zeta_i(t) + cF \left(\sum_{j=0}^{N} a_{ij}(\zeta_j(t) - \zeta_i(t)) \right) \tag{11}
$$

$$
+ c_0 \mathbf{sgn} \left(F \left(\sum_{j=0}^{N} a_{ij}(\zeta_j(t) - \zeta_i(t)) \right) \right) , i \in \mathcal{F}, \tag{12}
$$

where $\zeta_i(t) \in \mathbb{R}$ is defined as the state of the distributed observer of the leader's acceleration by the i-th follower CAV and $\zeta_0(t) = a_0(t)$, c and c_0 are the coupling gains, $K_1, K_2 \in \mathbb{R}^1$ are the control gains, $F \in \mathbb{R}$ is the observer gain, and $A = [a_{ij}]_{(N+1) \times (N+1)}$ is the adjacency matrix of graph $\mathcal{G}$, and $\mathbf{sgn}$ is the signum function defined component-wise, and $h_{is} - h_{0s} = (i - 0)d_c$ and $h_{is} - h_{js} = (i - j)d_c$ represents the desired distances between the CAVs i and 0 and the CAVs i and j, respectively. Here, $\mathcal{G}$ describes the communication topology among the $(N+1)$ CAVs at time $t \geq 0$ to specify the information flow topology. Specifically, the protocol (8) represents the control inputs, the condition (10) is the regulation information from the neighbors' position and speed, and the condition (12) is the distributed observer dynamics of the leader CAV and the compensation input of distributed estimation of the unknown jerk dynamics to provide a larger amount of acceleration compensation for the preceding CAVs.

Remark 5: The cooperative platooning tracking control protocols in this paper are also said to have structure $\mathcal{G}$ [54], where

uninstructed control protocols have a structure corresponding to the complete graph which requires communication between any part of CAVs, see [34] for examples. In this paper, we are only interested in the distributed control protocols using local information interaction under the directed structure G. Similar to [54], a direct communication link exists, which means that it is perfect in the sense of ignoring the effects on quantization, data dropouts, and time delays for simplicity.

Remark 6: Note that the employed distributed observer is very easy to implement when the position and velocity of neighbors can be received, which aims to propagate the information of the leader vehicle's acceleration rather than the general construction of states from measurements. Moreover, compared with the followers, the leader vehicle is disturbed by unknown jerk dynamics, so the distributed observer (12) will be invalid with $i = 0$ which implies that the leader CAV' dynamics will not be affected by the follower CAVs. In addition, since only a few follower CAVs can receive the information from the leader CAV, thus, tracking errors from neighboring vehicles are needed to construct the cooperative protocol. Notably, to capture the influence of unknown jerk dynamics on the leader CAV, the signum function is also used in the distributed observer (12).

It is noted that the traditional car-following model, as presented in [29], [49], [50], only considers how a driver responds to a single stimulus from other vehicles in some specific fashion. With the V2X infrastructure, we can collect the rich vehicle information to construct the cooperative perception which implies that we can able to use the cooperative information to respond to the multiple stimuli from other neighboring vehicles. Therefore, the dynamics $Y_i(v_i(t))$ can be designed by

$$Y_i(v_i(t)) = \sum_{j=0}^{N} a_{ij}[y(V_i(h_{ij}(t)) - v_i(t))], \quad (13)$$

where y is the sensitivity constant, $V_i(h_{ij}(t))$ is the nonlinear reaction function, or so-called the "optimal velocity function" (OVF), that captures the interactions between the CAVs i and j, and is associated with the specific average bumper-to-bumper headway [50]

$$V_i(h_{ij}(t)) = VC_1 + VC_2 \tanh(VC_3(h_{ij}(t)) - VC_4), \quad (14)$$

where VC_1, VC_2, VC_3, VC_4 are the positive constants, obtained from a calibration of the OVM with respect to empirical data [50].

Accordingly, the average bumper-to-bumper headway $h_{ij}(t)$ between the CAVs i and j can be designed by

$$h_{ij}(t) = (s_i(t) - s_j(t))/(i - j). \quad (15)$$

Remark 7: Different from the previous results [25], [26], [55] that assume either system dynamics with self-feedback terms of each node or the leader vehicle with a zero-input, the dynamics of the vehicle concerned in this paper are affected by the external unknown acceleration reference signals. What makes the problem interesting is that the inappropriate self-feedback terms of the CAVs may lead to more difficulties in coordinating controller design and platoon queue maintenance in an actual urban traffic environment. In addition, although the constant distance policy has the best potential to reduce the platoon length and thus

improve urban road throughput, the platoon stability still relies on the leader CAV's information. To solve these issues, the distributed observer design is developed to estimate the acceleration reference signals of the leader CAV using the local and directed information interaction, to improve the performance of cooperative platooning tracking control protocols on the resilience and robustness of platoon systems.

III. Cooperative platooning tracking control with unknown jerk dynamics

In this section, the cooperative platooning tracking control problem for the CAVs (2) and (3) under the unknown jerk dynamics will be solved by synchronizing distributed observers for all the CAVs and using our developed distributed protocols (8) - (12), where the feedback gains for the cooperative controller are considered to be fixed first; the optimal design of variable feedback gain will be discussed later. To obtain the main results, the following assumption and lemma are introduced.

Assumption 1: The leader CAV has one directed path to each follower CAV.

Remark 8: Note that Assumption 1 can be easily satisfied by using the V2V/V2X communication, which is reconfigurable on the basis of the actual communication capabilities at the design time because it only requires that the graph of communication topology satisfies the directed spanning tree condition. This is very different from the existing ACC [11], [12] and CACC [14]–[16] policy, in which the ideal control topology of a static and fixed communication pattern is usually considered [17], [18]. Therefore, we introduce the Assumption 1 to remove this limitation to consider a reconfigurable (not fixed) control topology at design-time to match the complex platoon characteristics.

Since the leader CAV has zero in-degree, according to [37], [56], the Laplacian matrix L of the communication topology $\mathcal{G}$ can be partitioned as

$$L = \begin{pmatrix} 0 & L_2 \\ L_0 & L_1 \end{pmatrix}, \quad (16)$$

where $L_2 \in 0_N^\top$, $L_0 \in \mathbb{R}^N$ and $L_1 \in \mathbb{R}^{N \times N}$.

Lemma 5: [56] With Assumption 1, there exists a positive vector $\theta = (\theta_1, \cdots, \theta_N)^\top \in \mathbb{R}^N$, such that

$$\Theta L_1 + L_1^\top \Theta > 0, \quad (17)$$

where $L_1^\top \theta = 1_N$, L_1 is defined in (16), and $\Theta = \mathbf{diag}\{1/\theta_1, \cdots, 1/\theta_N\}$.

Define $\theta_0 = \min_i(\theta_i), i \in \mathcal{F}$ and $\lambda_0 = \lambda_{\min}(\Theta L_1 + (L_1)^\top \Theta)$. Using the protocols (8) - (12), we have the following closed-loop

system:

$$
\begin{cases}
\dot{\xi}_i(t) = T_1 T_2^\top \xi_i(t) + T_2 \zeta_i(t) \\
\quad + cT_2 K_1 \left(\sum_{j=0}^{N} a_{ij}((s_j(t) - h_{js}) - (s_i(t) - h_{is})) \right) \\
\quad + cT_2 K_2 \left(\sum_{j=0}^{N} a_{ij}((v_j(t) - h_{jv}) - (v_i(t) - h_{iv})) \right) \\
\quad + T_3 \left(\sum_{j=0}^{N} a_{ij}(V_i(h_{ij}(t)) - v_i(t)) \right), \\
\dot{\xi}_0(t) = T_1 T_2^\top \xi_0(t) + T_2 \zeta_0(t),
\end{cases}
\tag{18}
$$

where $T_3 = [0, y]^\top$ and y is given by (13).

Furthermore, we have

$$
T_3 \left(\sum_{j=0}^{N} a_{ij}(V_i(h_{ij}(t)) - v_i(t)) \right)
$$

$$
= T_3 \left(\sum_{j=0}^{N} a_{ij}(V_i(h_{ij}(t)) - v_i(t) + v_0(t) - v_0(t)) \right)
$$

$$
= T_3 \left(\sum_{j=0}^{N} a_{ij}(V_i(h_{ij}(t)) - v_0(t)) \right) - T_3 \left(\sum_{j=0}^{N} a_{ij}(v_i(t) - v_0(t)) \right)
$$

Define $\delta_i(t) = \xi_i(t) - \xi_0(t) - h_i$ as the cooperative platooning tracking error, and $\varepsilon_i(t) = \zeta_i(t) - \zeta_0(t)$ as the estimation error, where $\delta(t) = [\delta_1^\top(t), \dots, \delta_N^\top(t)]^\top$, $\varepsilon(t) = [\varepsilon_1^\top(t), \dots, \varepsilon_N^\top(t)]^\top$, $h = [h_1^\top, \dots, h_N^\top]^\top$, $h_i = [h_{is}, h_{iv}]^\top$, and $i \in \mathcal{F}$. Then, we have

$$
\begin{aligned}
\dot{\xi}_i(t) =& T_1 T_2^\top \xi_i(t) + T_2 \zeta_i(t) \\
& + cT_2 K_1 \left(\sum_{j=0}^{N} a_{ij}((s_j(t) - h_{js}) - (s_i(t) - h_{is})) \right) \\
& + cT_2 K_2 \left(\sum_{j=0}^{N} a_{ij}((v_j(t) - h_{jv}) - (v_i(t) - h_{iv})) \right) \\
& + T_3 \left(\sum_{j=0}^{N} a_{ij}(V_i(h_{ij}(t)) - v_0(t)) \right) \\
& - T_3 \left(\sum_{j=0}^{N} a_{ij}((v_i(t) - v_0(t))) \right),
\end{aligned}
\tag{19}
$$

Remark 9: It is noted that control objective includes the $\lim_{t \to \infty} \|v_i(t) - v_0(t)\| = 0, \forall i \in \mathcal{F}$, that will be achieved by using the developed cooperative platooning tracking control protocols (8) - (12) with a distributed observer design under a directed communication topology. Therefore, the item $v_0(t)$ here is only used to describe the relative velocity error of cooperative platooning tracking, which does not require to be obtained for every CAV because v_0 is only accessible to a subset of CAVs in

our distributed protocols (8) - (12). With this design, the system dynamic (19) will represent the stable traffic flow by using our developed protocol.

Furthermore, we define $\bar{f}(t) = [f_1^\top(t), \dots, f_N^\top(t)]^\top$, where $f_i(t) = \sum_{j=0}^{N} a_{ij}(V_i(h_{ij}(t)) - v_0(t))$. Let $\xi_F(t) = [\xi_1^\top(t), \dots, \xi_N^\top(t)]^\top$, $\xi_L(t) = [\xi_0^\top(t), \dots, \xi_0^\top(t)]^\top$. Then, the tracking error system can be described by a compact form

$$
\begin{aligned}
\dot{\delta}(t) =& (I_N \otimes T_1 T_2^\top - c(L \otimes T_2 K)) \xi_F(t) - c(L \otimes T_2 K) h \\
& + (I_N \otimes T_2) \varepsilon(t) - (I_N \otimes T_1 T_2^\top) \xi_L(t) \\
& + (I_N \otimes T_4) \bar{f}(t) - (L_1 \otimes T_2 T_3^\top) \delta(t) \\
& - (L_1 \otimes T_2 T_3^\top) h \\
=& (I_N \otimes T_1 T_2^\top - c(L_1 \otimes T_2 K)) \delta(t) + (I_N \otimes T_2) \varepsilon(t) \\
& + (I_N \otimes T_4) \bar{f}(t) - (L_1 \otimes T_2 T_3^\top) \delta(t) \\
& + (I_N \otimes T_1 T_2^\top) h - (L_1 \otimes T_2 T_3^\top) h,
\end{aligned}
\tag{20}
$$

where $T_4 = \begin{bmatrix} 0 & 0 \\ y & 0 \end{bmatrix}$, $K = [K_1 \quad K_2]$.

Define $\zeta_F = [\zeta_1^\top(t), \dots, \zeta_N^\top(t)]^\top$ and $\zeta_L = [\zeta_0^\top(t), \dots, \zeta_0^\top(t)]^\top$. Accordingly, the estimation error dynamics can be given by

$$
\begin{aligned}
\dot{\varepsilon}(t) =& (I_N \otimes I_N) \zeta_F(t) - c(L \otimes F) \zeta(t) \\
& - c_0 (I_N \otimes I_N) \mathbf{sgn}((L \otimes F) \zeta(t)) \\
& - (I_N \otimes I_N) \zeta_L(t) - (I_N \otimes I_N) \rho(t) \\
=& (I_N \otimes I_N) \varepsilon(t) - c(L_1 \otimes F) \varepsilon(t) \\
& - c_0 (I_N \otimes I_N) \mathbf{sgn}((L_1 \otimes F) \varepsilon(t)) - (I_N \otimes I_N) \rho(t).
\end{aligned}
\tag{21}
$$

Remark 10: It follows from (20) and (21) that, the platoon dynamics in this paper are the functions of vehicle longitudinal dynamics denoted by $T_1 T_2^\top$, the traffic information flow denoted by the communication G and the matrix L_1, the nonlinear vehicle dynamics denoted by $\bar{f}(t)$, the unknown external input dynamics denoted by $\rho(t)$ and the feedback and observer gains denoted by the matrices K and F, which implies that the overall closed-loop system will be modified for the local vehicle closed-loop system under the information flow topology L. Therefore, different from the work [34], the stability of a platoon in this paper depends not only on its cooperative platooning tracking controller but also on the directed information flow topologies. Notably, the information flow in the current paper will be a fundamental condition for the platoon properties, i.e., stability and scalability.

Then, we present the first result for the cooperative platooning tracking control problem by developing a distributed estimation approach.

Theorem 1: Under Assumption 1, the cooperative platooning tracking control problem for the CAVs (2) and (3) is solved by the protocols (8) - (12) with proper feedback gains, identical inter-vehicle constraints (2), and the local information interaction if the following properties hold:

1) The platoon variable satisfies

$$
(I_N \otimes T_1 T_2^\top) h - (L_1 \otimes T_2 T_3^\top) h = 0, \tag{22}
$$

2) There exist two positive definite matrices P_0 and P such that

$$P_0 + P_0^\top - \omega\theta_0 P_0 F = -I_n, \tag{23}$$

$$T_1 T_2^\top P + P(T_1 T_2^\top)^\top - \omega\theta_0 T_2 T_2^\top + \lambda_0\theta_0 T_4(VC_2)DP$$
$$- \lambda_0\theta_0 T_2 T_3^\top P + \beta P < 0, \tag{24}$$

where $\omega > 0$, $c > \omega/\lambda_0$, $\lambda_0 = \lambda_{\min}(\Theta L_1 + L_1^\top\Theta)$, $\theta_0 = \min\theta_i$, $\theta = \{\theta_1, \ldots, \theta_N\}$, $L_1^\top\theta = 1_N$, L_1 is defined in (16), $\Theta = diag\{1/\theta_1, \ldots, 1/\theta_N\}$, $\beta > 0$, VC_2 is a scalar, and $D = \min(1/(i-j))$.

In this case, the parameters of protocols (8) - (12) will be determined as follows: $F = T^{-1}P_0$, $T = T^\top$, $K = T_2^\top P^{-1}$, and $c_0 \geq \bar{\rho}$.

Proof: Based on Lemma 5, the matrix L_1 is invertible. Thereby, the cooperative platooning tracking control problem for the CAVs (2) and (3) will be solved if and only if both error dynamics $\varepsilon_i(t)$ and $\delta_i(t)$ converge synchronously to zero. Then, consider the Lyapunov function as follows

$$\bar{V}(\varepsilon, \delta, t) = \bar{V}_1(\varepsilon, t) + \bar{V}_2(\varepsilon, \delta, t), \tag{25}$$

With $\bar{V}_1(\varepsilon, t) = 8\beta^{-1}\lambda_{\max}(T_2^\top P^{-1}T_2)\varepsilon^\top(t)(\Theta \otimes P_0)\varepsilon(t)$, $\bar{V}_2(\varepsilon, \delta, t) = \delta^\top(t)(\Theta \otimes P^{-1})\delta(t)$. The proof contains the following two parts.

Part I): the time derivative of $\bar{V}_1(\varepsilon, t)$ along the trajectories of system (21) takes

$$\dot{\bar{V}}_1(\varepsilon, t) \leq 8\beta^{-1}\lambda_{\max}(T_2^\top P^{-1}T_2)(\varepsilon^\top(t)(\Theta \otimes (P_0 + P_0^\top))$$
$$- 2c\Theta L_1 \otimes P_0 F)\varepsilon(t)$$
$$- 2c_0\varepsilon^\top(t)(\Theta \otimes P_0)\mathbf{sgn}((L_1 \otimes F)\varepsilon(t))$$
$$- 2\varepsilon^\top(t)(\Theta \otimes P_0)\rho(t). \tag{26}$$

Choose $c > \omega/\lambda_0$, where $\lambda_0 = \lambda_{\min}(\Theta L_1 + (L_1)^\top\Theta)$ and $\Theta = diag\{1/\theta_1, \ldots, 1/\theta_N\}$. Then, we have

$$\dot{\bar{V}}_1(\varepsilon, t) \leq 8\beta^{-1}\lambda_{\max}(T_2^\top P^{-1}T_2)(\varepsilon^\top(t)(\Theta \otimes (P_0 + P_0^\top))$$
$$- a((\Theta L_1 + (L_1)^\top\Theta) \otimes P_0 F))\varepsilon(t)$$
$$- 2c_0\varepsilon^\top(t)(\Theta \otimes P_0)\mathbf{sgn}((L_1 \otimes F)\varepsilon(t))$$
$$- 2\varepsilon^\top(t)(\Theta \otimes P_0)\rho(t))$$
$$\leq 8\beta^{-1}\lambda_{\max}(T_2^\top P^{-1}T_2)(\varepsilon^\top(t)(\Theta \otimes (P_0 + P_0^\top))$$
$$- a\lambda_0(I_N \otimes P_0 F))\varepsilon(t)$$
$$- 2c_0\varepsilon^\top(t)(\Theta \otimes P_0)\mathbf{sgn}((L_1 \otimes F)\varepsilon(t))$$
$$- 2\varepsilon^\top(t)(\Theta \otimes P_0)\rho(t))$$
$$\leq 8\beta^{-1}\lambda_{\max}(T_2^\top P^{-1}T_2)(\varepsilon^\top(t)(\Theta \otimes (P_0 + P_0^\top))$$
$$- \omega\theta_0(\Theta \otimes P_0 F))\varepsilon(t)$$
$$- 2c_0\varepsilon^\top(t)(\Theta \otimes P_0)\mathbf{sgn}((L_1 \otimes F)\varepsilon(t))$$
$$- 2\varepsilon^\top(t)(\Theta \otimes P_0)\rho(t), \tag{27}$$

where $\theta_0 = \min\theta_i, i \in \mathcal{F}$. Then, we consider the last two item in (27). With $F = T^{-1}P_0$, we have

$$\Delta = -2c_0\varepsilon^\top(t)(\Theta \otimes P_0)\mathbf{sgn}((L_1 \otimes F)\varepsilon(t))$$
$$- 2\varepsilon^\top(t)(\Theta \otimes P_0)\rho(t)$$
$$\leq -2c_0(\Theta \otimes I_N)((L_1)^{-1} \otimes T)\varepsilon^\top(t)(L_1 \otimes P_0 T^{-1})$$
$$\times \mathbf{sgn}((L_1 \otimes T^{-1}P_0)\varepsilon(t))$$
$$- 2(\Theta \otimes I_N)((L_1)^{-1} \otimes T)\varepsilon^\top(t)(L_1 \otimes P_0 T^{-1})\rho(t). \tag{28}$$

It is noted that $x^\top\mathbf{sgn}(x) = ||x||_1$. By using the boundedness of $\rho(t)$, we can have

$$\Delta \leq 2c_0(\Theta \otimes I_N)((L_1)^{-1} \otimes T)(||(L_1 \otimes P_0 T^{-1})\varepsilon(t)||_1)$$
$$- 2(\Theta \otimes I_N)((L_1)^{-1} \otimes T)\varepsilon^\top(t)(L_1 \otimes P_0 T^{-1})\rho(t)$$
$$\leq 2c_0(\Theta \otimes I_N)((L_1)^{-1} \otimes T)(||(L_1 \otimes P_0 T^{-1})\varepsilon(t)||_1)$$
$$+ 2(\Theta \otimes I_N)((L_1)^{-1} \otimes T)$$
$$\times ||\rho(t)||_\infty(||(L_1 \otimes P_0 T^{-1})\varepsilon(t)||_1)$$
$$\leq 2(c_0 - \bar{\rho})(\Theta \otimes I_N)((L_1)^{-1} \otimes T)(||(L_1 \otimes P_0 T^{-1})\varepsilon(t)||_1). \tag{29}$$

Let $c_0 \geq \bar{\rho}$. Then, we have $\Delta \leq 0$. By using (23) and the Schur complement lemma, we have

$$\dot{\bar{V}}_1(\varepsilon, t) \leq -8\beta^{-1}\varepsilon^\top(t)(\Theta \otimes T_2^\top P^{-1}T_2)\varepsilon(t). \tag{30}$$

Part II): Letting $h_{ij}^*(t)$ represents the steady headway between two neighboring CAVs and $V_i(h_{ij}^*(t))$ is the optimal velocity function under uniform traffic flow which satisfy $\lim_{t\to\infty} h_{ij}^*(t) = d_c$ and $\lim_{t\to\infty} V_i(h_{ij}^*(t)) = v_0$. Since $V_i(h_{ij}(t)) = V_i(h_{ij}^*(t)) +$

$V_i^{'}(h_{ij}(t))(h_{ij}(t) - h_{ij}^*(t))$, we have

$$
\sum_{j=0}^{N} a_{ij}(V_i(h_{ij}(t)) - v_0(t))
$$

$$
= \left(\sum_{j=0}^{N} a_{ij}(V_i(h_{ij}(t)) - V_i(h_{ij}^*(t)) + V_i(h_{ij}^*(t)) - v_0(t)) \right)
$$

$$
= \sum_{j=0}^{N} a_{ij}(V_i(h_{ij}(t)) - V_i(h_{ij}^*(t)) + \sum_{j=0}^{N} a_{ij}(V_i(h_{ij}^*(t)) - v_0(t))
$$

$$
= \sum_{j=0}^{N} a_{ij}(V_i^{'}(h_{ij}(t))(h_{ij}(t) - h_{ij}^*(t)) + \sum_{j=0}^{N} a_{ij}(V_i(h_{ij}^*(t)) - v_0(t))
$$

$$
\leq \sum_{j=0}^{N} a_{ij}(VC_2)(h_{ij}(t) - d_c) - \sum_{j=0}^{N} a_{ij}(VC_2)(h_{ij}^*(t) - d_c)
$$

$$
+ \sum_{j=0}^{N} a_{ij}(V_i(h_{ij}^*(t)) - v_0(t))
$$

$$
\leq \sum_{j=0}^{N} a_{ij}(VC_2)\left(\frac{s_i(t) - s_j(t) - (i-j)d_c}{i-j} \right)
$$

$$
- \sum_{j=0}^{N} a_{ij}(VC_2)(h_{ij}^*(t) - d_c) + \sum_{j=0}^{N} a_{ij}(V_i(h_{ij}^*(t)) - v_0(t)) \tag{31}
$$

Therefore, with the condition (22), the time derivative of $\bar{V}_2(\varepsilon, \delta, t)$ along the trajectories of system (20) takes

$$
\dot{\bar{V}}_2(\varepsilon, \delta, t) = \Delta_1 + \Delta_2 + \Delta_3
$$
$$
\Delta_3 = \delta^\top(t)(\Theta \otimes (P^{-1}T_1T_2^\top + (T_1T_2^\top)^\top P^{-1}))\delta(t)
$$
$$
- 2c\delta^\top(t)(\Theta L_1 \otimes P^{-1}T_2K)\delta(t)
$$
$$
+ 2\delta^\top(t)(\Theta L_1 \otimes P^{-1}T_4(VC_2)D)\delta(t)
$$
$$
- 2\delta^\top(t)(\Theta L_1 \otimes P^{-1}T_2T_3^\top)\delta(t)
$$
$$
+ 2\delta^\top(t)(\Theta \otimes P^{-1}T_2)\varepsilon(t). \tag{32}
$$

where $D = \min(1/(i-j))$, $\lim_{t\to\infty} \Delta_1 = 0$ and $\lim_{t\to\infty} \Delta_2 = 0$ due to $\lim_{t\to\infty} h_{ij}^*(t) = d_c$ and $\lim_{t\to\infty} V_i(h_{ij}^*(t)) = v_0$.

Substituting $K = T_2^\top P^{-1}$ into (32) yields

$$
\Delta_3 = \delta^\top(t)(\Theta \otimes (P^{-1}T_1T_2^\top + (T_1T_2^\top)^\top P^{-1}))\delta(t)
$$
$$
- 2c\delta^\top(t)(\Theta L_1 \otimes P^{-1}T_2T_2^\top P^{-1})\delta(t)
$$
$$
+ 2\delta^\top(t)(\Theta L_1 \otimes P^{-1}T_4(VC_2)D)\delta(t) \tag{33}
$$
$$
- 2\delta^\top(t)(\Theta L_1 \otimes P^{-1}T_2T_3^\top)\delta(t)
$$
$$
+ 2\delta^\top(t)(\Theta \otimes P^{-1}T_2)\varepsilon(t).
$$

Let $\tilde{\varepsilon}(t) = (\tilde{\varepsilon}_1^\top(t), \ldots, \tilde{\varepsilon}_N^\top(t))^\top$, where $\tilde{\varepsilon}_i(t) = P^{-1}\delta_i(t)$, $i \in \mathcal{F}$. Then, $\delta(t) = (I_N \otimes P)\tilde{\varepsilon}(t)$. It follows from (33) that

$$
\Delta_3 = \tilde{\varepsilon}^\top(t)(\Theta \otimes (T_1T_2^\top P + P(T_1T_2^\top)^\top))\tilde{\varepsilon}(t)
$$
$$
- 2c\tilde{\varepsilon}^\top(t)(\Theta L_1 \otimes T_2T_2^\top)\tilde{\varepsilon}(t)
$$
$$
+ 2\tilde{\varepsilon}^\top(t)(\Theta L_1 \otimes T_4(VC_2)DP)\tilde{\varepsilon}(t) \tag{34}
$$
$$
- 2\tilde{\varepsilon}^\top(t)(\Theta L_1 \otimes T_2T_3^\top P)\tilde{\varepsilon}(t)
$$
$$
+ 2\delta^\top(t)(\Theta \otimes P^{-1}T_2)\varepsilon(t).
$$

Noting that $c > \omega/\lambda_0$, where $\lambda_0 = \lambda_{\min}(\Theta L_1 + L_1^\top \Theta)$ and $\Theta = diag\{1/\theta_1, \ldots, 1/\theta_N\}$. Using (24) and the Schur complement lemma, we have

$$
\Delta_3 \leq - \beta\tilde{\varepsilon}_i^\top(t)(I_N \otimes P)\tilde{\varepsilon}_i(t) + 2\delta^\top(t)(\Theta \otimes P^{-1}T_2)\varepsilon(t)
$$
$$
= - \beta\delta^\top(t)(\Theta \otimes P^{-1})\delta(t) + 2\delta^\top(t)(\Theta \otimes P^{-1}T_2)\varepsilon(t). \tag{35}
$$

Thus, it follows from (25), (30), (31) and (35) that

$$
\lim_{t\to\infty} \dot{V}(\varepsilon, \delta, t) \leq \begin{pmatrix} \varepsilon \\ \delta \end{pmatrix}^\top \begin{pmatrix} \Omega_{11} & \Omega_{12} \\ * & \Omega_{22} \end{pmatrix} \begin{pmatrix} \varepsilon \\ \delta \end{pmatrix} \triangleq \psi^\top \Omega \psi, \tag{36}
$$

where $\Omega_{11} = -8\beta^{-1}(\Theta \otimes T_2^\top P^{-1}T_2)$, $\Omega_{12} = 2(\Theta \otimes T_2^\top P^{-1})$, and $\Omega_{22} = -\beta(\Theta \otimes P^{-1})$. It is not difficult to obtain that $\Omega_{11} < 0$, $\Omega_{22} < 0$ and $\Omega_{11} - \Omega_{12}\Omega_{22}^{-1}\Omega_{12}^\top = \frac{\Omega_{11}}{2} < 0$, and which is Schur equivalent to $\Omega < 0$. Then, $\dot{V}(\varepsilon_i, \delta_i, t)$ is bounded since $\lim_{t\to\infty} \dot{V}(\varepsilon_i, \delta_i, t) < 0$. Accordingly, $\varepsilon_i(t), \delta_i(t)$ are bounded as $t \to \infty$, and further $\dot{\varepsilon}_i(t), \dot{\delta}_i(t)$ and $\ddot{\delta}_i(t)$ are also bounded for (20), (21) and (25). For $\dot{V}(\varepsilon_i, \delta_i, t)$ in (26) and (32), we can conclude that $\ddot{V}(\varepsilon_i, \delta_i, t)$ is bounded. With Barbalat's lemma, we have $\dot{V}(\varepsilon_i, \delta_i, t) \to 0$ as $t \to \infty$. Furthermore, using Squeeze Theorem, it is resulting that both error dynamics $\varepsilon_i(t)$ and $\delta_i(t)$ converge synchronously to the origin as $t \to \infty$. Therefore, the cooperative platooning tracking control problem (6) is solved by the protocols (8) - (12). The proof is complete.

∎

Remark 11: This section develops a cooperative platooning tracking control protocol to ensure the desired safety distance among the CAVs, which allows each CAV to track its leader by using local information interaction and a car-following model. Specifically, the protocols (8) - (12) can be constructed if the conditions (22) - (24) are solvable for the given positive scalars ω, c, c_0, and β. It is noted that the selections of ω, c, c_0, and β do not influence the qualitative results given in Theorem 1. That is, ω, c, c_0, and β are free positive scalars in (22) - (24). However, a larger β will lead to a high gain feedback, which does not affect the asymptotic consensus behaviors of the platoon system, but could affect the transient behaviors or consensus rate which will be discussed below.

IV. Cooperative platooning tracking control with unknown jerk dynamics under intermittent optimization feedback gains

A general framework for the cooperative platooning tracking control problem for the CAVs (2) and (3) with the proper distributed estimation and compensation is presented in Sections III. Based on the results, we can design a cooperative tracking controller for the CAVs to ensure safe cruising. However, due to the cost constraints and the maneuverability demands for the dynamic response of the vehicle control, we would like to realize the cooperative platooning tracing control with an optimal control cost and minimum optimization calculations, which requires a new optimization design and a novel intermittent sampling condition of the feedback gain.

Consensually, to ensure that the velocity and acceleration estimation are within the given admissible range, the following constraints are first imposed

$$
\begin{aligned}
&v_{0,\min} \leq v_0(t) \leq v_{0,\max}, \\
&a_{0,\min} \leq a_0(t) \leq a_{0,\max}, \\
&v_{i,\min} \leq v_i(t) \leq v_{i,\max}, \\
&a_{0,\min} \leq \zeta_i(t) \leq a_{0,\max}, i \in \mathcal{F},
\end{aligned} \tag{37}
$$

where $v_{i,\min}$ and $v_{i,\max}$ are the known minimum and maximum speed limits, and $a_{i,\min}$ and $a_{i,\max}$ are the known minimum and maximum acceleration. Similarly, all the nonidentical acceleration/deceleration bounds for each CAV are assumed to be pre-specified and known. Different from the constraints in Subsection III, vehicle diversity here is considered owing to the nonidentical driveline performance.

We now would like to consider a sequence $[0,T_1), [T_1,T_2), \ldots, [T_k,T_{k+1}), k \in \mathbb{N}$, where $T_0 := 0$. For each interval $[T_k,T_{k+1})$, there exists another finite partition, $\{[T_{k,q}, T_{k,q+1}) \subseteq [T_k,T_{k+1}) | q \in \{0,\ldots,\bar{q}_k\} \in \mathbb{N} \wedge T_{k,0} := T_k \wedge T_{k,\bar{q}_{k+1}} = T_{k+1}\}$. Consider that the feedback gains of the interval $[T_k,T_{k+1})$, $K_{1,k}(t)$, $K_{2,k}(t)$ are chosen to be piecewise constants, where there exists an instant $\hat{q}_k \in \{0,...,\bar{q}_k\}$ (which will be designed later to minimize the total number of discrete time interval optimization) such that for all $t \in [T_{k,q}, T_{k,q+1})$, $0 \leq q < \hat{q}_k$, $K_1(t) = K_1(T_{k,q})$, $K_2(t) = K_2(T_{k,q})$, and for all $\hat{t} \in [T_{k,\hat{q}_k}, T_{k+1})$, $K_1(\hat{t}) = K_1(T_{k,s})$, $K_2(\hat{t}) = K_2(T_{k,s})$, where $T_{k,s}$ be the last sampling at $t \in [T_{k,q}, T_{k,\hat{q}_k})$. Then, for $q < \hat{q}_k$,

we design the following protocols

$$
u_i(T_{k,q}) = \zeta_i(T_{k,q}) + \hat{u}(T_{k,q}, K_1(T_{k,q}), K_2(T_{k,q})) \tag{38}
$$

$$
\hat{u}(T_{k,q}, K_1(T_{k,q}), K_2(T_{k,q})) \tag{39}
$$

$$
= cK_1(T_{k,q}) \Bigg(\sum_{j=0}^{N} a_{ij}((s_j(T_{k,q}) - h_{js}) \tag{40}
$$

$$
- (s_i(T_{k,q}) - h_{is})) \Bigg)
$$

$$
+ cK_2(T_{k,q}) \Bigg(\sum_{j=0}^{N} a_{ij}((v_j(T_{k,q}) - h_{jv}) \tag{41}
$$

$$
- (v_i(T_{k,q}) - h_{iv})) \Bigg), \tag{42}
$$

$$
\dot{\zeta}_i(T_{k,q}) = \zeta_i(t) + cF \left(\sum_{j=0}^{N} a_{ij}(\zeta_j(t) - \zeta_i(t)) \right) \tag{43}
$$

$$
+ c_0 \mathbf{sgn} \left(F \left(\sum_{j=0}^{N} a_{ij}(\zeta_j(t) - \zeta_i(t)) \right) \right), \tag{44}
$$

where $K_1(T_{k,q}) \in \mathbb{R}^1$ and $K_2(T_{k,q}) \in \mathbb{R}^1$ are the feedback gains. Similarly, the condition (42) represents the optimal regulation information from the neighbors, and the condition (44) denotes the distributed observer dynamics of the leader CAV and formulates an idea of applying a large compensation input of distributed estimation of the unknown jerk dynamics.

Remark 12: In this section, an optimization design of the feedback gain and an intermittent sampling condition is given in (38) - (44) to address the cost constraints and the maneuverability demands for the dynamic response of the vehicle control, aiming to improve the driving smoothness and comfort. It is noted that the optimization design and the intermittent sampling condition are only for the feedback gains $K_1(T_{k,q})$ and $K_2(T_{k,q})$, which does not change the communication among CAVs. Since the leader CAV exists the unknown jerk dynamics, to ensure safety, we here do not consider a sampling observer for the leader's acceleration; that is, maintaining the observer gain F for all the follower CAVs to handle the emergency. Therefore, the stability analysis is given again when the form of observer (44) is the same as that of observer (12) for the reader to understand.

The aim here is to find a $\hat{q}_i$ as small as possible, which can sufficiently guarantee the stability of CAVs (2) and (3) and maintain the minimum energy computation. Therefore, following [57], [58], we now formulate an intermittent optimization problem in

each time interval $[T_{k,q}, T_{k,q+1})$, shown as follows:

$$
\begin{aligned}
[K_1(T_{k,q}), K_2(T_{k,q})] :=&arg \min_{[K_1,K_2]} J_{i,T_{k,q}} \\
=&\sum_{i=0}^{N} \Bigg(\|\xi_i(t) - h_i - \xi_0(t)\|_Q^2 + \|\zeta_i(T_{k,q}) \\
&+ \hat{u}(T_{k,q}, K_1(T_{k,q}), K_2(T_{k,q}))\|_R^2 \Bigg), \\
& Subject \ to \ (2), (3), (6), (7), (37) - (44),
\end{aligned}
$$
(45)

where $\xi_i(t)$ and $\xi_0(t)$ are the sampling states, and $u_{i,T_{k,q}}$ is the control input for the follower CAV i, $i \in \mathcal{F}$, at the time $T_{k,q}$, $Q > 0$ and $R > 0$ are the symmetric weighting matrices, and J_i is the optimization cost.

Then, we introduce the following assumption:

Assumption 2: The optimization (45) can be solved within $[T_{k,q}, T_{k,q+1})$ for each $q \in \{0, ..., \hat{q}_k\}$. And $K_{1,0}$, $K_{2,0}$ are either computed in the last sub-interval of $[T_{k-1}, T_k)$, when $k \geq 1$, or offline computed, when $k = 0$.

Remark 13: Assumption 2 implies that the CAVs can have the access to the optimal feedback gains over some discontinuous time intervals owing to the discrete digital sampling signals of vehicular equipment and V2X infrastructure. Under this assumption, we consider that for all $[T_{k,\hat{q}_k}, T_{k+1})$, $K_1(t) = K_{1,t_{\hat{q}_k}}$, $K_2(t) = K_{2,t_{\hat{q}_k}}$, to reduce the amount of computation. In addition, the optimization problem (45) is not just about saving energy, it's a design approach about how to achieve the stability of the platoon systems with the shortest amount of computation under the condition of each step optimization. Different from [57], [58], we here consider achieving the goal with the minimization number of optimization methods.

In the following, we will present the sampling condition and analyze the stability of the CAVs under the intermittent optimization problem. Then, for $t \in [T_{k,q}, T_{k,\hat{q}_k})$, using the protocols (38) - (44), the closed-loop system is given by:

$$
\begin{cases}
\dot{\xi}_i(t) =T_1 T_2^\top \xi_i(t) + T_2 \zeta_i(t) \\
\qquad + cT_2 K_1(T_{k,q}) \left(\sum_{j=0}^{N} a_{ij}((s_j(t) - h_{js}) - (s_i(t) - h_{is})) \right) \\
\qquad + cT_2 K_2(T_{k,q}) \left(\sum_{j=0}^{N} a_{ij}((v_j(t) - h_{jv}) - (v_i(t) - h_{iv})) \right) \\
\qquad + T_3(\sum_{j=0}^{N} a_{ij}(V_i(h_{ij}(t)) - v_i(t))), \\
\dot{\xi}_0(t) =T_1 T_2^\top \xi_0(t) + T_2 \zeta_0(t),
\end{cases}
$$
(46)

Define $\delta_i(t) = \xi_i(t) - \xi_0(t) - h_i$ as the tracking error, $\varepsilon_i(t) = \zeta_i(t) - \zeta_0(t)$ as the estimate error, where $\delta(t) = [\delta_1^\top(t), \ldots, \delta_N^\top(t)]^\top$, $\varepsilon(t) = [\varepsilon_1^\top(t), \ldots, \varepsilon_N^\top(t)]^\top$, $h = [h_1^\top, \ldots, h_N^\top]^\top$, $h_i = [h_{ix}, h_{iv}]^\top$, and $K(T_{k,q}) = [K_1(T_{k,q}) K_2(T_{k,q})]$. Then, for $t \in [T_{k,q}, T_{k,\hat{q}_k})$, the tracking error

systems can be written as a compact form

$$
\begin{aligned}
\dot{\delta}(t) =&(I_N \otimes T_1 T_2^\top - c(L_1 \otimes T_2 K(T_{k,q})))\delta(t) \\
&+ (I_N \otimes T_2)\varepsilon(t) + (I_N \otimes T_4)\bar{f}(t) \\
&- (L_1 \otimes T_2 T_3^\top)\delta(t) + (I_N \otimes T_1 T_2^\top)h - (L_1 \otimes T_2 T_3^\top)h.
\end{aligned}
$$
(47)

where $\bar{f}(t) = [f_i^\top(t), \ldots, f_N^\top(t)]^\top$, $f_i(t) = \sum_{j=0}^{N} a_{ij}(V_i(h_{ij}(t)) - v_0(t))$.

Thus, the estimate error are given by

$$
\begin{aligned}
\dot{\varepsilon}(t) =&(I_N \otimes I_N)\varepsilon(t) - c(L_1 \otimes F)\varepsilon(t) \\
&- c_0(I_N \otimes I_N)\mathbf{sgn}((L_1 \otimes F)\varepsilon(t)) - (I_N \otimes I_N)(\rho(t)).
\end{aligned}
$$
(48)

Similarly, for $\hat{t} \in [T_{k,\hat{q}_k}, T_{k+1})$, the tracking error is as follows:

$$
\begin{aligned}
\dot{\delta}(\hat{t}) =&(I_N \otimes T_1 T_2^\top - c(L_1 \otimes T_2 K(T_{k,s})))\delta(\hat{t}) \\
&+ (I_N \otimes T_2)\varepsilon(\hat{t}) + (I_N \otimes T_4)\bar{f}(\hat{t}) \\
&- (L_1 \otimes T_2 T_3^\top)\delta(\hat{t}) + (I_N \otimes T_1 T_2^\top)h - (L_1 \otimes T_2 T_3^\top)h.
\end{aligned}
$$
(49)

Thereby, the estimate error can be given by

$$
\begin{aligned}
\dot{\varepsilon}(\hat{t}) =&(I_N \otimes I_N)\varepsilon(\hat{t}) - c(L_1 \otimes F)\varepsilon(\hat{t}) \\
&- c_0(I_N \otimes I_N)\mathbf{sgn}((L_1 \otimes F)\varepsilon(\hat{t})) - (I_N \otimes I_N)(\rho(\hat{t})).
\end{aligned}
$$
(50)

Then, we present the following result.

Theorem 2: Under Assumptions 1 and 2, the cooperative platooning tracking control optimization problem for the CAVs (2) and (3) is solved by the protocols (38) - (44) with intermittent optimization feedback gains, nonidentical inter-vehicle constraints (37), and local information interaction if the following properties hold:

1) The conditions (7) and (22) hold,
2) The following optimal problem with LMI and the cost constraints has a feasible solution

$$
\min \gamma_{T_{k,q}}
$$
(51)

$$
Subject \ to : (37),
$$

$$
T_1 T_2^\top W_{T_{k,q}} + W_{T_{k,q}}(T_1 T_2^\top)^\top - \omega\theta_0\gamma_{T_{k,q}} T_2 T_2^\top H_{T_{k,q}}
$$
(52)

$$
+ \lambda_0\theta_0 T_4(VC_2)DW_{T_{k,q}}
$$

$$
- \lambda_0\theta_0 T_2 T_3^\top W_{T_{k,q}} + \beta W_{T_{k,q}} < 0,
$$
(53)

$$
T_1 T_2^\top W_{T_{k,q}} + W_{T_{k,q}}(T_1 T_2^\top)^\top - \omega\theta_0\gamma_{T_{k,q}} T_2 T_2^\top H_{T_{k,q}}
$$
(54)

$$
+ \lambda_0\theta_0 T_4(VC_2)DW_{T_{k,q}}
$$

$$
- \lambda_0\theta_0 T_2 T_3^\top W_{T_{k,q}} - \lambda W_{T_{k,q}} < 0,
$$
(55)

$$
\bar{V}_{T_{k,q}} < \gamma_{T_{k,q}},
$$
(56)

$$
W_{T_{k,q}} > 0,
$$
(57)

$$
H_{T_{k,q}} > 0.
$$
(58)

where $\gamma_{T_{k,q}}$ is the cost and $\bar{V}_{T_{k,q}}$ is the energy function.

3) The sampling time internals satisfy

$$\frac{\hat{q}_k}{2\lambda_{\min}(P_0)} - \frac{\left(-8\beta^{-1} + 4\lambda^{-1}\right)}{8\beta^{-1}\lambda_{\min}(P_0)}(T_{k+1} - T_k - \hat{q}_k) > 0,$$
(59)

where $\omega > 0$ are $\beta > 0$ two scalars.

In this case, the parameters of protocols (38) - (44) will be determined as follows: $K_{T_{k,q}} = T_2^\top \gamma_{T_{k,q}} W_{T_{k,q}}^{-1} H_{T_{k,q}}$, and $F = T^{-1}P_0$, $T = T^\top$, $c_0 \geq \bar{\rho}$, $c > \omega/\lambda_0$ and the other parameters are the same as that of Theorem 1.

Proof: To analyze the stability of the closed-loop systems, we define the following Lyapunov function

$$\bar{V}(\varepsilon, \delta, t) = \bar{V}_1(\varepsilon, t) + \bar{V}_2(\varepsilon, \delta, t), t \in [T_k, T_{k+1}),$$
(60)

with $\bar{V}_1(\varepsilon, t) = 8\beta^{-1}\lambda_{\max}(T_2^\top P_{T_{k,q}}T_2)\varepsilon^\top(t)(\Theta \otimes P_0)\varepsilon(t)$, $\bar{V}_2(\varepsilon, \delta, t) = \delta^\top(t)(\Theta \otimes P_{T_{k,q}}^{-1})\delta(t)$, where $P_{T_{k,q}} = \gamma_{T_{k,q}}^{-1} W_{T_{k,q}}$, $W_{T_{k,q}}$ is the positive definite matrix. To ensure the mobility of the CAVs, we consider that the acceleration estimation has a fixed feedback gain F. This implies that the acceleration estimation only schedules the estimated state at each time interval $T_{k,q}$. That is, for each $t \in [T_k, T_{k+1})$, we only need to analyze $\bar{V}_2(\varepsilon, \delta, t)$. In fact, the matrix $W_{T_{k,q}}$ is the solution of LMI (53) for $t \in [T_{k,q}, T_{k,\hat{q}_k})$ and $W_{T_{k,q}} = W_{T_{k,s}}$ which will be held for $\hat{t} \in [T_{k,\hat{q}_k}, T_{k+1})$. The specific proof contains the following two parts.

Part I): For $t \in [T_{k,q}, T_{k,\hat{q}_k})$, with the condition (22), the time derivative of $\bar{V}_2(\varepsilon, \delta, t)$ along the trajectories of system (47) takes

$$\dot{\bar{V}}_2(\varepsilon, \delta, t) = \Delta_1 + \Delta_2 + \Delta_3$$
$$\Delta_3 = \delta^\top(t)(\Theta \otimes (P_{T_{k,q}}^{-1}T_1T_2^\top + (T_1T_2^\top)^\top P_{T_{k,q}}^{-1}))\delta(t)$$
$$- 2c\delta^\top(t)(\Theta L_1 \otimes P_{T_{k,q}}^{-1}T_2K_{T_{k,q}})\delta(t)$$
$$+ 2\delta^\top(t)(\Theta L_1 \otimes P_{T_{k,q}}^{-1}T_4(VC_2)D)\delta(t)$$
$$- 2\delta^\top(t)(\Theta L_1 \otimes P_{T_{k,q}}^{-1}T_2T_3^\top)\delta(t)$$
$$+ 2\delta^\top(t)(\Theta \otimes P_{T_{k,q}}^{-1}T_2)\varepsilon(t).$$
(61)

where $\lim_{t\to\infty}\Delta_1 = 0$ and $\lim_{t\to\infty}\Delta_2 = 0$ due to $\lim_{t\to\infty}h_{ij}^*(t) = d_c$ and $\lim_{t\to\infty}V_i(h_{ij}^*(t)) = v_0$. Ideally, the proof of Theorem 2 will be the same as that in Theorem 1 if we can prove that $\Delta_3 \leq -\beta\delta^\top(t)(\Theta \otimes P_{T_{k,q}}^{-1})\delta(t) + 2\delta^\top(t)(\Theta \otimes P_{T_{k,q}}^{-1}T_2)\varepsilon(t)$ for $t \in [T_{k,q}, T_{k,\hat{q}_k})$. For simplify, we only consider the optimal profile below

$$\Delta = \delta^\top(t)(\Theta \otimes (P_{T_{k,q}}^{-1}T_1T_2^\top + (T_1T_2^\top)^\top P_{T_{k,q}}^{-1}))\delta(t)$$
$$- 2c\delta^\top(t)(\Theta L_1 \otimes P_{T_{k,q}}^{-1}T_2K_{T_{k,q}})\delta(t)$$
$$+ 2\delta^\top(t)(\Theta L_1 \otimes P_{T_{k,q}}^{-1}T_4(VC_2)D)\delta(t)$$
$$- 2\delta^\top(t)(\Theta L_1 \otimes P_{T_{k,q}}^{-1}T_2T_3^\top)\delta(t),$$
(62)

which implies that we only need to prove $\Delta < -\beta\delta^\top(t)(\Theta \otimes P_{T_{k,q}}^{-1})\delta(t)$. Therefore, following [57], [58], we define the following cost constraint

$$J_{T_{k,q}} \leq \bar{V}_{T_{k,q}} \leq \delta^\top(t)(\Theta \otimes P_{T_{k,q}}^{-1})\delta(t).$$
(63)

By defining an upper bound $\bar{V}_{T_{k,q}} \leq \gamma_{T_{k,q}}$, we get

$$J_{T_{k,q}} \leq \gamma_{T_{k,q}}.$$
(64)

If the condition (63) holds, the ellipsoid $\Omega(\Theta \otimes P_{T_{k,q}}^{-1}, \gamma_{T_{k,q}})$ will be a convergence domain for each iteration calculation. Define $W_{T_{k,q}} = \gamma_{T_{k,q}}P_{T_{k,q}}$, $H_{T_{k,q}} = M_{T_{k,q}}P_{T_{k,q}}$. Then, substituting $K_{T_{k,q}} = T_2^\top M_{T_{k,q}}$ into (61) yields

$$\Delta = \delta^\top(t)(\Theta \otimes (P_{T_{k,q}}^{-1}T_1T_2^\top + (T_1T_2^\top)^\top P_{T_{k,q}}^{-1}))\delta(t)$$
$$- 2c(\delta^\top(t))(\Theta L_1 \otimes P_{T_{k,q}}^{-1}T_2T_2^\top M_{T_{k,q}})\delta(t)$$
$$+ 2\delta^\top(t)(\Theta L_1 \otimes P_{T_{k,q}}^{-1}T_4(VC_2)D)\delta(t)$$
$$- 2\delta^\top(t)(\Theta L_1 \otimes P_{T_{k,q}}^{-1}T_2T_3^\top)\delta(t).$$
(65)

By choosing $c > \omega/\lambda_0$, where $\lambda_0 = \lambda_{\min}(\Theta L_1 + (L_1^\top)\Theta)$ and $\Theta = diag\{1/\theta_1, \ldots, 1/\theta_N\}$, we have

$$\Delta \leq \delta^\top(t)(\Theta \otimes (P_{T_{k,q}}^{-1}T_1T_2^\top + (T_1T_2^\top)^\top P_{T_{k,q}}^{-1}))\delta(t)$$
$$- \omega\theta_0\delta^\top(t)(\Theta \otimes P_{T_{k,q}}^{-1}T_2T_2^\top M_{T_{k,q}})\delta(t)$$
$$+ \lambda_0\theta_0\delta^\top(t)(\Theta \otimes P_{T_{k,q}}^{-1}T_4(VC_2)D)\delta(t)$$
$$- \lambda_0\theta_0\delta^\top(t)(\Theta \otimes P_{T_{k,q}}^{-1}T_2T_3^\top)\delta(t).$$
(66)

Let $\tilde{\varepsilon}(t) = (\tilde{\varepsilon}_1^\top(t), \ldots, \tilde{\varepsilon}_N^\top(t))^\top$, where $\tilde{\varepsilon}_i(t) = \gamma_{T_{k,q}}^{-1}P_{T_{k,q}}^{-1}\delta_i(t)$, $i \in \mathcal{F}$. Then, $\delta(t) = (I_N \otimes \gamma_{T_{k,q}}P_{T_{k,q}})\tilde{\varepsilon}(t)$. It thus follows from (66) that

$$\Delta \leq \tilde{\varepsilon}^\top(t)(\Theta \otimes (\gamma_{T_{k,q}}T_1T_2^\top P_{T_{k,q}}\gamma_{T_{k,q}}$$
$$+ \gamma_{T_{k,q}}P_{T_{k,q}}(T_1T_2^\top)^\top \gamma_{T_{k,q}}))\tilde{\varepsilon}(t)$$
$$- \omega\theta_0\tilde{\varepsilon}^\top(t)(\Theta \otimes \gamma_{T_{k,q}}T_2T_2^\top M_{T_{k,q}}P_{T_{k,q}}\gamma_{T_{k,q}})\tilde{\varepsilon}(t)$$
$$+ \lambda_0\theta_0\tilde{\varepsilon}^\top(t)(\Theta \otimes \gamma_{T_{k,q}}T_4(VC_2)DP_{T_{k,q}}\gamma_{T_{k,q}})\tilde{\varepsilon}(t)$$
$$- \lambda_0\theta_0\tilde{\varepsilon}^\top(t)(\Theta \otimes \gamma_{T_{k,q}}T_2T_3^\top P_{T_{k,q}}\gamma_{T_{k,q}})\tilde{\varepsilon}(t).$$
(67)

Let $W_{T_{k,q}} = \gamma_{T_{k,q}}P_{T_{k,q}}$. Then, we have

$$\Delta \leq \tilde{\varepsilon}^\top(t)(\Theta \otimes (\gamma_{T_{k,q}}T_1T_2^\top W_{T_{k,q}} + \gamma_{T_{k,q}}W_{T_{k,q}}(T_1T_2^\top)^\top))\tilde{\varepsilon}(t)$$
$$- \omega\theta_0(\tilde{\varepsilon}^\top(t))(\Theta \otimes \gamma_{T_{k,q}}T_2T_2^\top M_{T_{k,q}}W_{T_{k,q}})\tilde{\varepsilon}(t)$$
$$+ \lambda_0\theta_0\tilde{\varepsilon}^\top(t)(\Theta \otimes \gamma_{T_{k,q}}T_4(VC_2)DW_{T_{k,q}})\tilde{\varepsilon}(t)$$
$$- \lambda_0\theta_0\tilde{\varepsilon}^\top(t)(\Theta \otimes \gamma_{T_{k,q}}T_2T_3^\top W_{T_{k,q}})\tilde{\varepsilon}(t).$$
(68)

Together with $H_{T_{k,q}} = M_{T_{k,q}}P_{T_{k,q}}$, we can obtain

$$\Delta \leq (\tilde{\varepsilon}^\top(t))(\Theta \otimes (\gamma_{T_{k,q}}T_1T_2^\top W_{T_{k,q}} + \gamma_{T_{k,q}}W_{T_{k,q}}(T_1T_2^\top)^\top))\tilde{\varepsilon}(t)$$
$$- \omega\theta_0(\tilde{\varepsilon}^\top(t))(\Theta \otimes \gamma_{T_{k,q}}T_2T_2^\top H_{T_{k,q}}\gamma_{T_{k,q}})\tilde{\varepsilon}(t)$$
$$+ \lambda_0\theta_0\tilde{\varepsilon}^\top(t)(\Theta \otimes \gamma_{T_{k,q}}T_4(VC_2)DW_{T_{k,q}})\tilde{\varepsilon}(t)$$
$$- \lambda_0\theta_0\tilde{\varepsilon}^\top(t)(\Theta \otimes \gamma_{T_{k,q}}T_2T_3^\top W_{T_{k,q}})\tilde{\varepsilon}(t).$$
(69)

Using (53) and the Schur complement lemma, we have

$$\Delta \leq -\gamma_{T_{k,q}}\beta(\tilde{\varepsilon}(t))^\top(\Theta \otimes W_{T_{k,q}})\tilde{\varepsilon}(t).$$
(70)

That is

$$\Delta \leq -\beta(\delta^\top(t))(\Theta \otimes P_{T_{k,q}}^{-1})\delta(t).$$
(71)

which is follows from (30), (31), (60) and (71) that

$$\dot{V}(\varepsilon,\delta,t) \leq \begin{pmatrix} \varepsilon \\ \delta \end{pmatrix}^\top \begin{pmatrix} \tilde{\Omega}_{11} & \tilde{\Omega}_{12} \\ * & \tilde{\Omega}_{22} \end{pmatrix} \begin{pmatrix} \varepsilon \\ \delta \end{pmatrix} + \Delta_1 + \Delta_2 \tag{72}$$
$$\triangleq \psi^\top \tilde{\Omega} \psi + \Delta_1 + \Delta_2,$$

where $\tilde{\Omega}_{11} = -8\beta^{-1}(\Theta \otimes T_2^\top P_{T_{k,q}}^{-1} T_2)$, $\tilde{\Omega}_{12} = 2(\Theta \otimes T_2^\top P_{T_{k,q}}^{-1})$, and $\tilde{\Omega}_{22} = -\beta(\Theta \otimes P_{T_{k,q}}^{-1})$. Using Lemma 4, it is not difficult to obtain that $\tilde{\Omega}_{11} < 0$, $\tilde{\Omega}_{22} < 0$ and

$$\begin{aligned} \tilde{\Omega}_{11} - \tilde{\Omega}_{12}\tilde{\Omega}_{22}^{-1}\tilde{\Omega}_{12}^\top &= \frac{\tilde{\Omega}_{11}}{2} \\ &= -4\beta^{-1}(\Theta \otimes T_2^\top P_{T_{k,q}}^{-1} T_2) \\ &< 0, \end{aligned} \tag{73}$$

which is Schur equivalent to $\tilde{\Omega} = \begin{bmatrix} \tilde{\Omega}_{11} & \tilde{\Omega}_{12} \\ * & \tilde{\Omega}_{22} \end{bmatrix} < 0$.

Part II): For the $\hat{t} \in [T_{k,\hat{q}_k}, T_{k+1})$, based on the dynamics (49) and (50), using a similar calculation, LMI (55) condition and the Schur complement lemma, we have

$$\Delta \leq \lambda(\delta^\top(\hat{t}))(\Theta \otimes P_{T_{k,s}}^{-1})\delta(\hat{t}), \tag{74}$$

which draws from (30), (32), (60) and (74) that

$$\dot{V}(\varepsilon,\delta,\hat{t}) \leq \begin{pmatrix} \varepsilon \\ \delta \end{pmatrix}^\top \begin{pmatrix} \Omega_{11} & \Omega_{12} \\ * & \Omega_{22} \end{pmatrix} \begin{pmatrix} \varepsilon \\ \delta \end{pmatrix} + \Delta_1 + \Delta_2 \tag{75}$$
$$\triangleq \psi^\top \Omega \psi + \Delta_1 + \Delta_2,$$

where $\Omega_{11} = -8\beta^{-1}(\Theta \otimes T_2^\top P_{T_{k,s}}^{-1} T_2)$, $\Omega_{12} = 2(\Theta \otimes T_2^\top P_{T_{k,s}}^{-1})$, and $\Omega_{22} = \lambda(\Theta \otimes P_{T_{k,s}}^{-1})$. Using Lemma 4, it is not difficult to obtain that $\Omega_{11} < 0$, $\Omega_{22} < 0$ and

$$\begin{aligned} \Omega_{11} - \Omega_{12}\Omega_{22}^{-1}\Omega_{12}^\top &= \frac{\Omega_{11}}{2} \\ &= (-8\beta^{-1} + 4\lambda^{-1})(\Theta \otimes T_2^\top P_{T_{k,s}}^{-1} T_2). \end{aligned} \tag{76}$$

According to (31), (59), (73), and (76), we can get

$$\bar{V}(\varepsilon,\delta,T_{k+1}) < e^{-\frac{\hat{q}_k}{2\lambda_{\max}(P_0)} + (\frac{-8\beta^{-1}+4\lambda^{-1}}{8\beta^{-1}\lambda_{\min}(P_0)})(T_{k+1}-T_k-\hat{q}_k)+\hat{\Delta}} \times \bar{V}_1(T_k), \tag{77}$$

where $\hat{\Delta}$ is a small difference due to the bounded dynamics Δ_1 and Δ_2 and satisfies $\lim_{t\to\infty}\hat{\Delta} = 0$.

Therefore, it follows the condition (77) that

$$\bar{V}(\varepsilon,\delta,T_{k+1}) < e^{-\vartheta}\bar{V}_1(T_k), \tag{78}$$

where $\vartheta > 0$ is a sufficiently small positive scalar. Since the time intervals $[T_k, T_{k+1})$ are uniformly bounded, $\bar{V}(\varepsilon,\delta,t)$ is bounded. Similar to the proof in Theorem 1, we have that $\dot{\bar{V}}(\varepsilon_i,\delta_i,t)$ and $\ddot{\bar{V}}(\varepsilon_i,\delta_i,t)$ are also bounded. With Barbalat's lemma, we have $\dot{\bar{V}}(\varepsilon_i,\delta_i,t) \to 0$ as $t \to \infty$. Furthermore, using Squeeze Theorem, it is resulting that both error dynamics $\varepsilon_i(t)$ and $\delta_i(t)$ converge synchronously to the origin as $t \to \infty$. Thus, it concludes that we can prove the reasonable conditions (63) and (64). The rest

of the proof is the same as that in Theorem 1. This completes the proof.

∎

Remark 14: Similar to Theorem 1, the selections of ω, c, c_0, β, and ϑ do not influence the qualitative results given in Theorem 2, which implies that ω, c, c_0, β, and ϑ are free positive scalars in the solutions of (53) - (55). Differently, a larger β, in this case, will not only affect the transient behaviors but also the sampling time internals so it must be a trade-off between the sampling cost and consensus rate.

Remark 15: Generally, the stability analysis of the platoon vehicles in the ACC and CACC strategies is also called single-vehicle stability (or platoon stability/plant stability) and stability over vehicles (or string stability), respectively [59]. Although local stability analysis of car-following models has been conducted since 1959 [60], due to its relative simplicity compared with string stability analysis, it did not attract as much attention as that of string stability analysis in the literature. Notably, unlike local stability, to be string stable requires that the perturbation strictly attenuates for each leader-follower pair as it propagates away from the first leader [36]. Specifically, an important feature is that a car-following model is able to easily recover from small disturbances in real traffic and return to a steady car-following model state over time. Thus, different from the existing works [15], [17], [28], [35] that mainly focus on the constant cruising speed for the leader CAV, for the first time, this paper develops an integrated model consisting of consensus-based information and car-following model under the unknown jerk profile, in which the consensus protocol can provide a free design for the communication information exchanged and the optimal velocity model can provide the perception information via V2X communication. Specifically, compared with the works [34], [40], [41], we can provide the distributed control and real-time optimal design for the feedback gains to improve the applicability and extensibility of the system in complex traffic environments.

Remark 16: In this paper, we aim to obtain the cooperative platooning tracking control by developing the distributed control $u_i(t)$ with the proper feedback gains and local information interaction, where the communication topology among the CAVs is free-design but has a directed spanning tree. Compared with the work [40], the cooperative platooning tracking control in our paper does not need the extra global variables, which is easier to implement for the real traffic environment because there are no special constraints on the upper bounds of the unknown jerk dynamics. In fact, the jerk dynamics of the leader CAV in the actual traffic control will be affected by the unknown traffic network conditions, e.g., stop-and-go, or sudden acceleration caused by unpredicted traffic congestion so it has to observe the dynamics of the leader CAV in real-time. Therefore, our paper develops a distributed and real-time optimal framework to address the cooperative platooning tracking control problem under a more general and practical traffic control scenario.

V. Simulations

The effectiveness of the proposed cooperative platooning tracking algorithms is illustrated in this section through two study cases. The CAVs are defined by the dynamics (2) and (3). We consider a single lane in the simulations.

Example 1: We consider a CAV system consisting of seven CAVs under the directed communication topology with the following Laplacian matrix

$$L = \begin{bmatrix} 0 & 0 & 0 & 0 & 0 & 0 & 0 \\ -1 & 1 & 0 & 0 & 0 & 0 & 0 \\ 0 & -1 & 1 & 0 & 0 & 0 & 0 \\ 0 & 0 & -1 & 1 & 0 & 0 & 0 \\ 0 & 0 & 0 & -1 & 1 & 0 & 0 \\ 0 & 0 & 0 & 0 & -1 & 1 & 0 \\ 0 & 0 & -1 & 0 & 0 & -1 & 2 \end{bmatrix}.$$

In this simulation, the cooperative platooning tracking protocols (8) - (12) are constructed according to Theorem 1. It is noted that the parameters of the protocols (8) - (12) rely on the solutions to (23) and (24). By choosing $\omega = 1$, we have $c > \omega/\lambda_0 = 9.1575$. Then, take $c = 9.2 > 9.1575$. Letting $VC_1 = 6.75 m/s, VC_2 = 7.91 m/s, VC_3 = 0.13 m^{-1}, VC_4 = 1.59$ (see [30]). Define the formation information as $h_0 = [0,0], h_1 = [-30,0], h_2 = [-60,0], h_3 = [-90,0], h_4 = [-120,0], h_5 = [-150,0], h_6 = [-180,0]$. Then, we have $d_c = 30m$. We consider the identical constraints of acceleration and velocity as $a_{\min} = -5 m/s^2, a_{\max} = 3 m/s^3, v_{\min} = 7 m/s, v_{\max} = 20 m/s$. Specifically, motivated by [61], we here consider the following Sine jerk model-like unknown signals for the leader CAV

$$\rho(t) = \begin{cases} -0.01, & 0 \leq t \leq 10, \\ 2.5 \times \sin(0.2 \times t), & 10 < t \leq 20, \\ 2.5 \times \cos(0.2 \times t), & 20 < t \leq 30, \\ 0.01, & 30 < t. \end{cases}$$

Clearly, $\hat{\rho} = 2.5$.

Remark 17: The jerk dynamics have been developed in the identification of driver intention [62], the identification of aggressive drivers [63], the detection of jerks in safety-critical events [64], the analysis in rail vehicle dynamics [65], and the optimal eco-driving for autonomous vehicles [41]. However, the jerk dynamics in the above works are assumed to be constant or different types of phases. Recently, an optimal jerk profile of bang-off-bang type for automated robots and machines was introduced in [66], where the specified jerk dynamics are a piecewise function with polynomial models. For traffic control, the piecewise performance of jerk dynamics has been studied in the trajectory planning and tracking for pedestrian-aware autonomous driving in urban environments [67], and the velocity planner for the online management of autonomous vehicles [68], where jerk dynamic is the trapezoidal trajectory as the polynomial models featuring an impulsive jerk profile. Notably, the trapezoidal trajectory will cause excessive stress on the actuators and mechanical structure engendered by step changes in acceleration as shown in [67], [68]. To this end, the rectangular-shaped jerk is adopted to weaken excessive stress from the trapezoidal trajectory. However, the trajectory has a shortcoming of jumps in jerk, and nonzero instantaneous jerks at the target points will lead to unexpected residual vibrations with accompanying extra settling time, which

deteriorates the positioning accuracy [66]. To further enhance the smoothness of the trajectory, the continuity of snap, or even higher-order derivatives, should be taken into account. However, the number of trajectory segments will increase exponentially along with the model order and hence can lead to a complicated algorithm for modeling the jerk dynamics with no available analytical solutions, which shows a remarkable negative effect on the computational efficiency and poses a challenge for the controller. Since the formulation of the trajectory profile and the scheduling procedure will become rather cumbersome as the polynomial model becomes smoother, in the exploration of new S-curve approaches, some investigations have attempted to devise motion profiles applying a trigonometric model to ensure the continuity of the jerk [66]. In fact, as pointed out in [36], all vehicles should decelerate smoothly and the time derivative of the acceleration function, i.e., the jerk, is finite at all times, which implies that the acceleration function is continuously differentiable in many cases. Motivated by [61], unlike the above piecewise function for a polynomial model, we here consider a piecewise function for applying a trigonometric model to ensure the continuity of the jerk and formulate the driving condition in urban environments

In the simulation, by letting $c_0 \geq \hat{\rho}$, we can analyze the cooperative platooning tracking behaviors for the CAVs in the absence and presence of effects of a car-following model, respectively, such as $y = \{0, 0.3, 0.5\} s^{-1}$. Taking the platooning tracking speed as $\beta = 0.1$, according to Theorem 1, we can obtain $F = 2.4142$ and $K = \{[2.3432, 5.6905], [3.2193, 7.5110], [5.9320, 12.9989]\}$. To show the platoon performance, first, we analyze the cooperative platooning tracking control for the closed-loop system (3) with the leader (2) under the protocols (8) - (12) without the car-following model, i.e., setting the parameter $y = 0$. Define the average observer error as $Error_0(t) = \frac{1}{6}\sqrt{\sum_{i=1}^{6} \|\zeta_i(t) - a_0(t)\|^2}$ and the distributed observer tracking errors as $Error_{0i}(t) = \sqrt{\|\zeta_i(t) - a_0(t)\|^2}$, $i = 1, \ldots, 6$. The average and distributed observer errors for seven CAVs are shown in Fig. 1, where all the observer errors will converge to zero, which implies that the estimation of all the follower CAVs for the unknown jerk dynamics of the leader CAV has been achieved. Then, the velocity and displacement trajectories of the closed-loop system (3) with the leader CAV (2) under the protocols (8) - (12) are shown in Figs. 2. (a) - (b), respectively. Define the average tracking error as $Error(t) = \frac{1}{6}\sqrt{\sum_{i=1}^{6} \|s_i(t) - s_0(t)\|^2}$ and the distributed tracking errors as $Error_i(t) = \sqrt{\|s_i(t) - s_0(t)\|^2}$, $i = 1, \ldots, 6$. Thereby, the average and distributed tracking distances for seven CAVs are shown in Fig. 2 (c), which implies that the cooperative platooning tracking queue is indeed achieved among the CAVs. Now, we show the cooperative platooning tracking control under the different car-following model profiles. Notably, the distributed observer protocol is not affected by the car-follower model. Therefore, by setting the parameters $y = \{0.3, 0.5\}$, the velocity and displacement trajectories of the closed-loop system (3) with the leader CAV (2) under the protocols (8) - (12) are shown in Figs. 3. (a) - (b) and Figs. 4. (a) - (b), respectively. Specifically, the tracking distances of seven CAVs are shown in Fig. 3. (c) and Fig. 4. (c), which imply that the cooperative platooning tracking queues are indeed achieved. From the velocity and

14

displacement trajectories, we can see that the cooperative platoon behaviors among the CAVs are achieved earlier when each CAV has a car-following model, which is also reflected in the tracking distances of the CAVs because the driver has better driving sensitivity. In addition, we introduce three evaluation indicators, i.e., mean, variance, and standard deviation(SD), to show the platoon performance for the average vehicle tracking error under the different car-following models, where $y = 0$, $y = 0.3$ and $y = 0.5$ are respectively the Model 1, Model 2 and Model 3, as shown in the Table 1). It is shown that the mean of the average tracking error of all CAVs fluctuates very little, i.e., about 0.9% increase, but the variance and SD of the average tracking error decrease significantly as y increases, i.e., about 6% and 3% decreases, as shown in Fig. (5) and Table 1. This implies that the platoon performance of the proposed new car-following model compared with the existing formation tracking [40] or the platoon control [17], [25], [26], [28], [32]–[35] (only consider the cooperative information, not cooperative perception, as Model 1 shown in Table 1) has better traffic performance, i.e., the smaller variance and SD of average vehicle tracking error, the higher vehicle efficiency and driving safety;
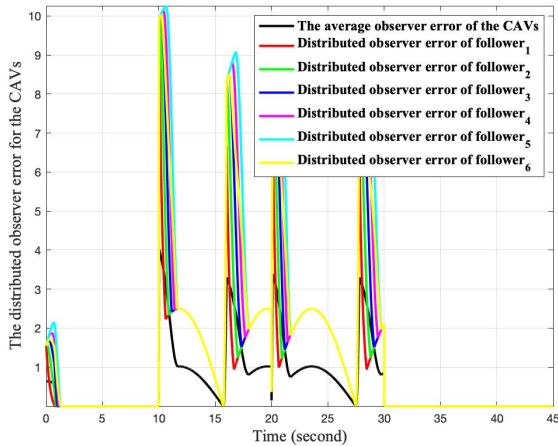

Fig. 1. Swarm distributed observers for the unknown jerk dynamics of the leader CAV under the protocols (12) without the car-following model.

TABLE I
THE AVERAGE TRACKING ERROR OF ALL CAVS(M)

	Mean	Variance	SD	%	%	%
Model 1	45.2614	33.2111	5.7629	(+)0.0%	(+)0.0%	(+)0.0%
Model 2	45.5826	32.7908	5.7263	(+)0.7%	(-)1.3%	(-)0.6%
Model 3	45.6905	31.2016	5.5858	**(+)0.9%**	**(-)6.0%**	**(-)3.0%**

Example 2: In this example, we consider the cooperative platooning tracking control for seven CAVs with optimal feedback gains. Specifically, motivated by [69], we here consider the following Harmonic jerk model-like unknown signals for the leader CAV

$$
\rho(t) = \begin{cases}
-0.01, & 0 \le t \le 20, \\
1.4 \times (1 - \cos(0.2 \times t)), & 20 < t \le 30, \\
1.4 \times (1 - \sin(0.2 \times t)), & 30 < t \le 40, \\
0.01, & 30 < t.
\end{cases}
$$

Clearly, $\hat{\rho} = 2.8$. The other system dynamics and the communication topology are the same as that in Example 1. Different from the Example 1 that employs the fixed feedback gain K, the feedback gain $K(t)$ will be calculated online from zero to an optimal value. The constraints of acceleration and velocity for the i-th vehicle are considered as $a_{0,\min} = -5m/s^2, a_{0,\max} = 3m/s^2$, $a_{i,\min} = (7 + 0.1 \times i)m/s^2, a_{i,\max} = (20 + 0.1 \times i)m/s^2$, $i = 0, \ldots, 6$, respectively. The other parameters are the same as that in Example 1. With $\beta = 0.2$, $\lambda = 0.1$, and $\lambda_{\min}(P_0) = 2.4142$, it is assumed that the sample and optimal time are activated when $t \in [T_k, T_{k+0.2})s$ and the fixed feedback gain is to be taken in $t \in [T_{k+0.2}, T_{k+1})s$. Then, the cooperative platooning tracking for the CAV (3) with the leader CAV (2) under protocols (38) - (44) will be achieved. Similarly, by setting the parameter $y = 0$, the average and distributed observers errors for seven CAVs are shown in Fig. 6, where all the observer errors will converge to zero, which implies that the estimation of all the follower CAVs for the unknown jerk dynamics of the leader CAV has been achieved. Then, the velocity and displacement trajectories of the closed-loop system (3) with the leader CAV (2) under protocols (38) - (44) are shown in Figs. 7. (a) and (b), respectively. Besides, the tracking distances of seven CAVs are shown in Fig. 7. (c), which shows that the cooperative platooning tracking queue is indeed held under the optimized feedback gains. Then, we present the cooperative platooning tracking control under the car-following model profiles. By setting the different reaction parameters $y = \{0.3, 0.5\}$, the velocity and displacement trajectories of the closed-loop system (3) with the leader CAV (2) under the protocols (38) - (44) are shown in Figs. 8. (a) - (b) and Figs. 9. (a) - (b), respectively. Accordingly, the tracking distances of seven CAVs are shown in Fig. 8. (c) and Fig. 9. (c), which show that the cooperative platooning tracking queues are indeed achieved. In addition, from the velocity and displacement trajectories, we can also see that the cooperative platoon behaviors among the CAVs are achieved earlier when each CAV has a car-following model and optimal feedback gains, which is particularly shown in the tracking distances of the CAVs. It is also shown that the cooperative platooning tracing control with optimized feedback gains can provide better platoon performance compared with the developed distributed control framework as shown in Example 1. Similarly, we also consider three evaluation indicators to show the platoon performance for the average vehicle tracking error. Clearly, the mean of the average tracking error of all CAVs changes very little, about 1.8%, but the variance and SD of the average tracking error also decrease significantly as y increases, about 22.2% and 11.8%, as shown in Fig. (5) and Table 2. This implies that under the identical condition (the optimization design and intermittent sampling condition of the feedback gain) the platoon performance of the proposed new car-following model compared with the existing formation tracking [40] or the platoon control [17], [25], [26], [28], [32]–[35], still has better traffic performance. Specifically, compared with the developed distributed
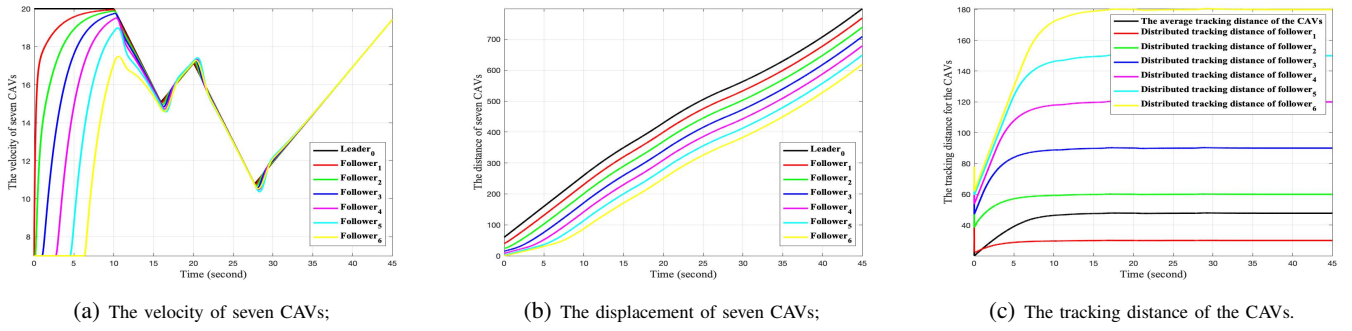
(a) The velocity of seven CAVs;

(b) The displacement of seven CAVs;

(c) The tracking distance of the CAVs.

Fig. 2. Swarm cooperative platooning tracking under the protocols (8) - (12) without the car-following model.

(a) The velocity of seven CAVs;
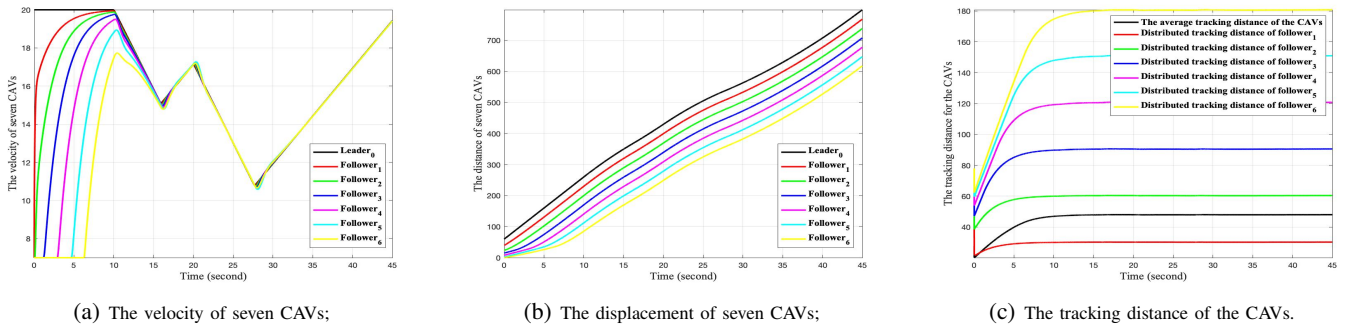

(b) The displacement of seven CAVs;

(c) The tracking distance of the CAVs.

Fig. 3. Swarm cooperative platooning tracking with the car-following model ($y = 0.3$) under the protocols (8) - (12).

(a) The velocity of seven CAVs;

(b) The displacement of seven CAVs;
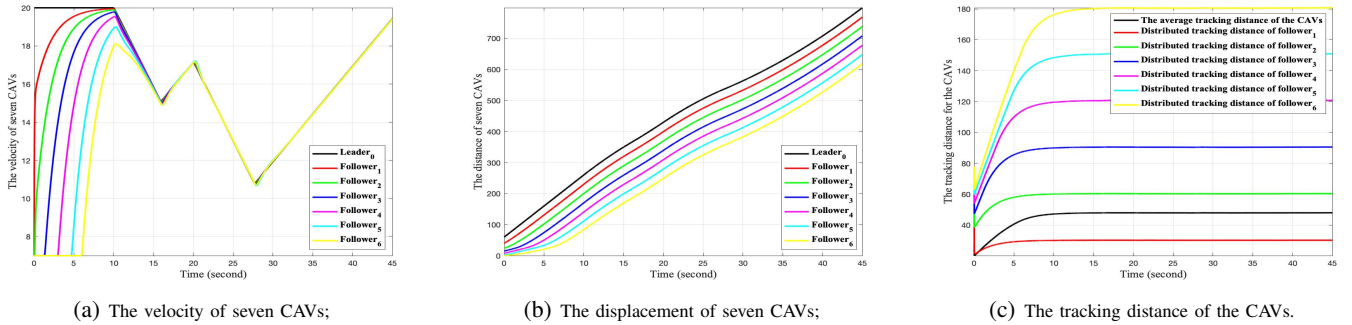

(c) The tracking distance of the CAVs.

Fig. 4. Swarm cooperative tracking with the car-following model ($y = 0.5$) under the control protocols (8)- (12).

control framework with a fixed feedback gain design as shown in Example 1, the optimization design and intermittent sampling condition of the feedback gain may provide more benefits, i.e., better traffic throughput and driving safety.

TABLE II
THE AVERAGE TRACKING ERROR OF ALL CAVS(M)

	Mean	Variance	SD	%	%	%
Model 1	45.2478	33.8229	5.8157	(+)0.0%	(+)0.0%	(+)0.0%
Model 2	45.8371	28.9330	5.3789	(+)1.3%	(-)14.5%	(-)7.5%
Model 3	46.0562	26.3071	5.1290	**(+)1.8%**	**(-)22.2%**	**(-)11.8%**

VI. Conclusions

So far, we have investigated the problem of cooperative platooning tracking control and optimization for the CAVs in a distributed framework with a leader CAV having unknown jerk dynamics and a nonlinear car-following model to provide the optimal velocity for each tracking CAV. The main contribution is to achieve the cooperative platooning tracking by designing a distributed control that consists of both the estimated dynamics and cooperative dynamics. Within this framework, the cooperative platooning tracking control problem can be regarded as the distributed estimation and compensation problem of the follower CAVs with optimal velocities for the leader CAV to reach the specified platoon queue. By introducing the distributed observer approach,
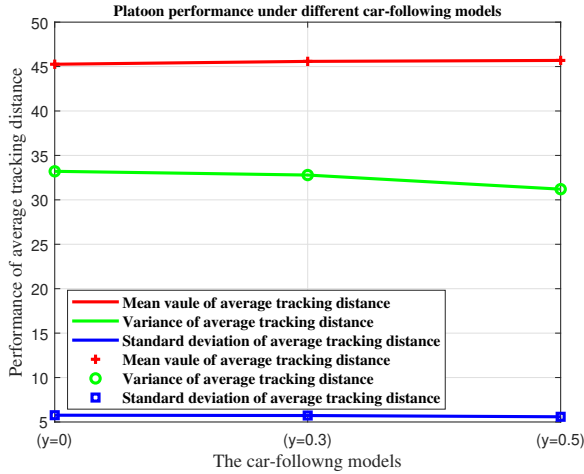
Fig. 5.   Platoon performances under different car-following models.
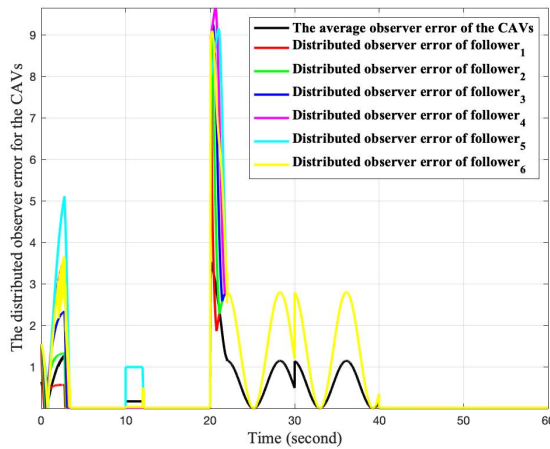

Fig. 6.   Swarm distributed observers for the unknown jerk dynamics of the leader CAV under the protocols (44) without the car-following model.

our theory and experimental results indicate that follower CAVs are able to track their leader with a safe inter-vehicle separation. Furthermore, the feedback control gain is optimized by using a robust control scheme. It is noted that, for some complex traffic scenarios, e.g., lane changes, the information exchange pattern may be time-varying owing to the communication distance or safety constraints both at run-time and design time. In this case, the dynamic topology of the exchanged weights should be considered at design time, which will affect the estimation and perception of all the follower CAVs for the unknown jerk dynamics of the leader CAVs. Specifically, the switching conditions for the time-varying communication topologies need to be investigated, which will be our future works.

In addition, although the constant distance headway can lead to the high traffic capacity, effectiveness and adaptability are still equally important. However, as [6] pointed out that maintaining a small gap among the vehicles may require aggressive throttling and braking, and may lead to suboptimal operation of the powertrain when the velocity profile is variable. Therefore,

how to design the proper constant time headway to enhance a high safety level at high speed and ensure traffic flow stability while improving the efficient movement of platoon CAVs with heterogeneous vehicle parameters will be developed in the future in virtue of the works [34], [40].

References

[1] L. Li, D. Wen, and D. Yao, "A survey of traffic control with vehicular communications," *IEEE Transactions on Intelligent Transportation Systems*, vol. 15, no. 1, pp. 425–432, 2014.

[2] K. C. Dey, A. Rayamajhi, M. Chowdhury, P. Bhavsar, and J. Martin, "Vehicle-to-vehicle (v2v) and vehicle-to-infrastructure (v2i) communication in a heterogeneous wireless network–performance evaluation," *Transportation Research Part C: Emerging Technologies*, vol. 68, pp. 168–184, 2016.

[3] X. Meng and C. G. Cassandras, "Optimal control of autonomous vehicles for non-stop signalized intersection crossing," in *2018 IEEE Conference on Decision and Control (CDC)*.   IEEE, 2018, pp. 6988–6993.

[4] Y. J. Zhang, A. A. Malikopoulos, and C. G. Cassandras, "Optimal control and coordination of connected and automated vehicles at urban traffic intersections," in *2016 American Control Conference (ACC)*.   IEEE, 2016, pp. 6227–6232.

[5] A. A. Malikopoulos, C. G. Cassandras, and Y. J. Zhang, "A decentralized energy-optimal control framework for connected automated vehicles at signal-free intersections," *Automatica*, vol. 93, pp. 244–256, 2018.

[6] J. Guanetti, Y. Kim, and F. Borrelli, "Control of connected and automated vehicles: State of the art and future challenges," *Annual Reviews in Control*, vol. 45, pp. 18–40, 2018.

[7] Y. Zheng, J. Ma, and L. Wang, "Consensus of hybrid multi-agent systems," *IEEE Transactions on Neural Networks and Learning Systems*, vol. 29, no. 4, pp. 1359–1365, 2018.

[8] B. Ning, Q.-L. Han, Z. Zuo, J. Jin, and J. Zheng, "Collective behaviors of mobile robots beyond the nearest neighbor rules with switching topology," *IEEE Transactions on Cybernetics*, vol. 48, no. 5, pp. 1577–1590, 2018.

[9] G. Wen and W. X. Zheng, "On constructing multiple lyapunov functions for tracking control of multiple agents with switching topologies," *IEEE Transactions on Automatic Control*, vol. 64, no. 9, pp. 3796–3803, 2019.

[10] B. Wang, W. Chen, and B. Zhang, "Semi-global robust tracking consensus for multi-agent uncertain systems with input saturation via metamorphic low-gain feedback," *Automatica*, vol. 103, pp. 363–373, 2019.

[11] A. Vahidi and A. Eskandarian, "Research advances in intelligent collision avoidance and adaptive cruise control," *IEEE Transactions on Intelligent Transportation Systems*, vol. 4, no. 3, pp. 143–153, 2003.

[12] G. J. Naus, R. P. Vugts, J. Ploeg, M. J. van De Molengraft, and M. Steinbuch, "String-stable cacc design and experimental validation: A frequency-domain approach," *IEEE Transactions on Vehicular Technology*, vol. 59, no. 9, pp. 4268–4279, 2010.

[13] J. Ploeg, B. T. Scheepers, E. Van Nunen, N. Van de Wouw, and H. Nijmeijer, "Design and experimental evaluation of cooperative adaptive cruise control," in *2011 14th International IEEE Conference on Intelligent Transportation Systems (ITSC)*.   IEEE, 2011, pp. 260–265.
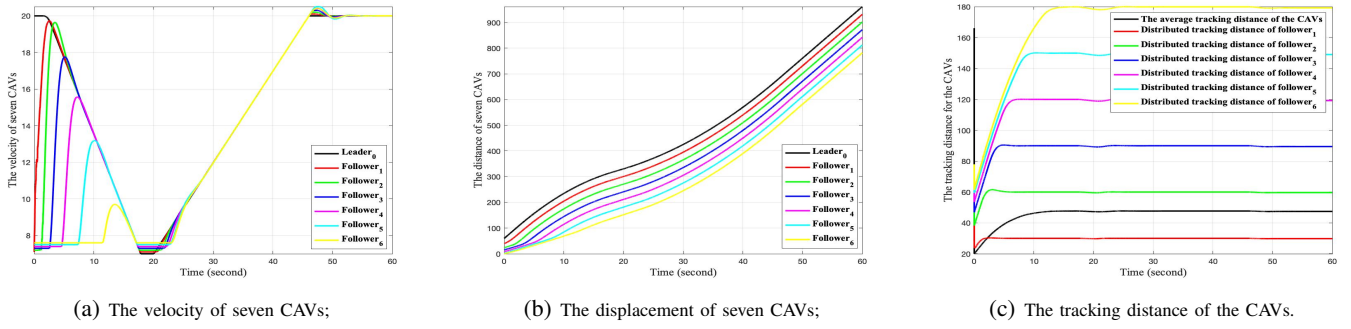
(a) The velocity of seven CAVs; (b) The displacement of seven CAVs; (c) The tracking distance of the CAVs.

Fig. 7. Swarm cooperative platooning tracking without the car-following model under the control protocols (38) - (44) having optimal feedback gains.

(a) The velocity of seven CAVs; (b) The displacement of seven CAVs; (c) The tracking distance of the CAVs.
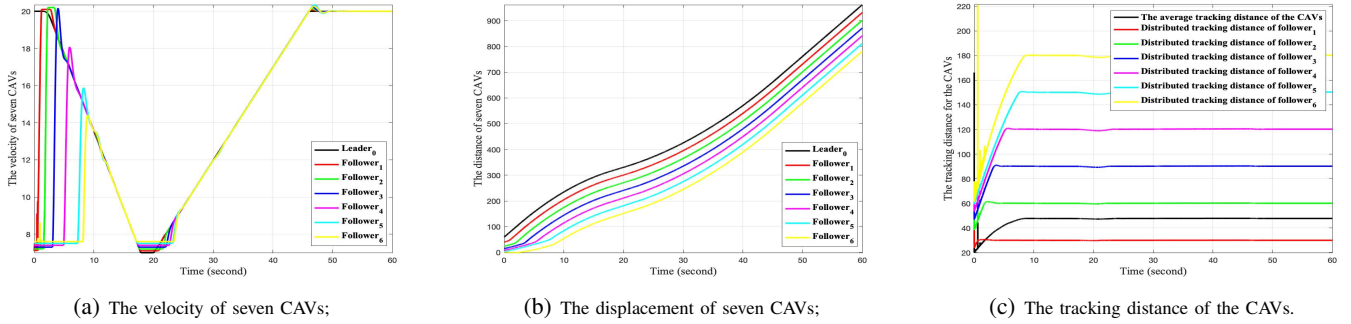
Fig. 8. Swarm cooperative platooning tracking with the car-following model ($y = 0.1$) under the control protocols (38) - (44) having optimal feedback gains.

(a) The velocity of seven CAVs; (b) The displacement of seven CAVs; (c) The tracking distance of the CAVs.
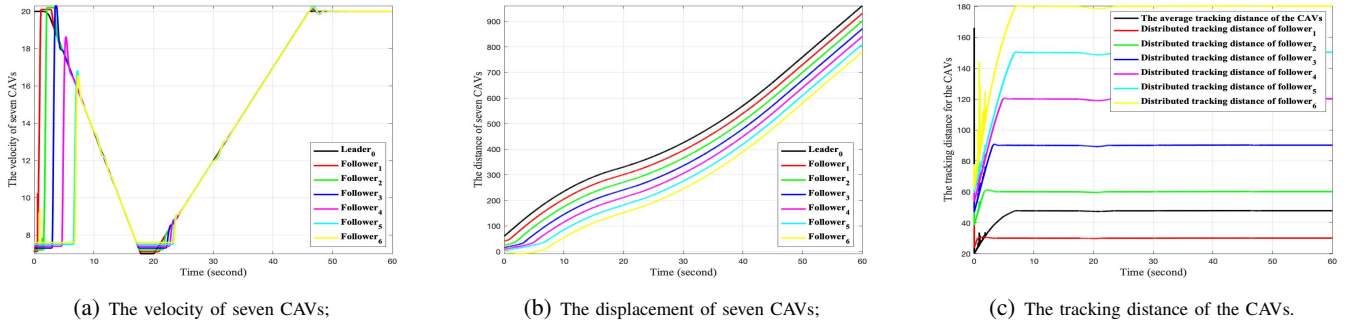
Fig. 9. Swarm cooperative platooning tracking with the car-following model ($y = 0.5$) under the control protocols (38) - (44) having optimal feedback gains.

[14] V. Milanés, S. E. Shladover, J. Spring, C. Nowakowski, H. Kawa-zoe, and M. Nakamura, "Cooperative adaptive cruise control in real traffic situations," *IEEE Transactions on Intelligent Transportation Systems*, vol. 15, no. 1, pp. 296–305, 2013.

[15] J. Ploeg, N. Van De Wouw, and H. Nijmeijer, "Lp string stability of cascaded systems: Application to vehicle platooning," *IEEE Transactions on Control Systems Technology*, vol. 22, no. 2, pp. 786–793, 2013.

[16] J. C. Zegers, E. Semsar-Kazerooni, J. Ploeg, N. van de Wouw, and H. Nijmeijer, "Consensus control for vehicular platooning with velocity constraints," *IEEE Transactions on Control Systems Technology*, vol. 26, no. 5, pp. 1592–1605, 2017.

[17] S. Santini, A. Salvi, A. S. Valente, A. Pescapé, M. Segata, and R. L. Cigno, "A consensus-based approach for platooning with interve-

hicular communications and its validation in realistic scenarios," *IEEE Transactions on Vehicular Technology*, vol. 66, no. 3, pp. 1985–1999, 2016.

[18] D. Jia and D. Ngoduy, "Platoon based cooperative driving model with consideration of realistic inter-vehicle communication," *Transportation Research Part C: Emerging Technologies*, vol. 68, pp. 245–264, 2016.

[19] M. Di Bernardo, A. Salvi, and S. Santini, "Distributed consensus strategy for platooning of vehicles in the presence of time-varying heterogeneous communication delays," *IEEE Transactions on Intelligent Transportation Systems*, vol. 16, no. 1, pp. 102–112, 2015.

[20] M. di Bernardo, P. Falcone, A. Salvi, and S. Santini, "Design, analysis, and experimental validation of a distributed protocol for platooning in the presence of time-varying heterogeneous delays,"
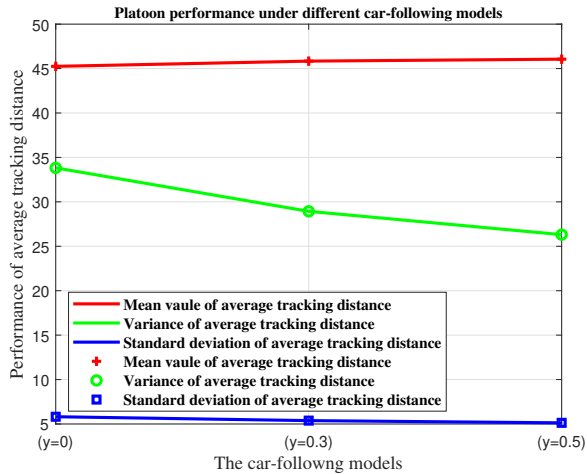
Fig. 10. Platoon performances under different car-following models.

IEEE Transactions on Control Systems Technology, vol. 24, no. 2, pp. 413–427, 2016.

[21] D. Jia and D. Ngoduy, "Enhanced cooperative car-following traffic model with the combination of v2v and v2i communication," *Transportation Research Part B: Methodological*, vol. 90, pp. 172–191, 2016.

[22] J. C. Zegers, E. Semsar-Kazerooni, J. Ploeg, N. van de Wouw, and H. Nijmeijer, "Consensus control for vehicular platooning with velocity constraints," *IEEE Transactions on Control Systems Technology*, vol. 26, no. 5, pp. 1592–1605, 2018.

[23] A. Salvi, S. Santini, and A. S. Valente, "Design, analysis and performance evaluation of a third order distributed protocol for platooning in the presence of time-varying delays and switching topologies," *Transportation Research Part C: Emerging Technologies*, vol. 80, pp. 360–383, 2017.

[24] R. Rajamani, *Vehicle dynamics and control*. Springer Science & Business Media, 2012.

[25] X. Dong, B. Yu, Z. Shi, and Y. Zhong, "Time-varying formation control for unmanned aerial vehicles: Theories and applications," *IEEE Transactions on Control Systems Technology*, vol. 23, no. 1, pp. 340–348, 2015.

[26] X. Dong and G. Hu, "Time-varying formation tracking for linear multiagent systems with multiple leaders," *IEEE Transactions on Automatic Control*, vol. 62, no. 7, pp. 3658–3664, 2017.

[27] B. Wang, J. Wang, B. Zhang, and X. Li, "Global cooperative control framework for multiagent systems subject to actuator saturation with industrial applications," *IEEE Transactions on Systems, Man, and Cybernetics Systems*, vol. 47, no. 7, pp. 1270–1283, 2017.

[28] B. Wang, J. Wang, B. Zhang, W. Chen, and Z. Zhang, "Leader–follower consensus of multivehicle wirelessly networked uncertain systems subject to nonlinear dynamics and actuator fault," *IEEE Transactions on Automation Science and Engineering*, vol. 15, no. 2, pp. 492–505, 2018.

[29] M. Bando, K. Hasebe, A. Nakayama, A. Shibata, and Y. Sugiyama, "Dynamical model of traffic congestion and numerical simulation," *Physical review E*, vol. 51, no. 2, p. 1035, 1995.

[30] Y. Li, L. Zhang, H. Zheng, X. He, S. Peeta, T. Zheng, and Y. Li, "Nonlane-discipline-based car-following model for electric vehicles in transportation-cyber-physical systems," *IEEE Transactions on Intelligent Transportation Systems*, vol. 19, no. 1, pp. 38–47, 2017.

[31] R. E. Wilson and J. A. Ward, "Car-following models: fifty years of linear stability analysis–a mathematical perspective," *Transportation Planning and Technology*, vol. 34, no. 1, pp. 3–18, 2011.

[32] F. Lin, M. Fardad, and M. R. Jovanovic, "Optimal control of vehicular formations with nearest neighbor interactions," *IEEE Transactions on Automatic Control*, vol. 57, no. 9, pp. 2203–2218, 2011.

[33] H. Hao and P. Barooah, "Stability and robustness of large platoons of vehicles with double-integrator models and nearest neighbor interaction," *International Journal of Robust and Nonlinear Control*, vol. 23, no. 18, pp. 2097–2122, 2013.

[34] S. Gong, J. Shen, and L. Du, "Constrained optimization and distributed computation based car following control of a connected and autonomous vehicle platoon," *Transportation Research Part B: Methodological*, vol. 94, pp. 314–334, 2016.

[35] S. Santini, A. Salvi, A. S. Valente, A. Pescapè, M. Segata, and R. L. Cigno, "Platooning maneuvers in vehicular networks: A distributed and consensus-based approach," *IEEE Transactions on Intelligent Vehicles*, vol. 4, no. 1, pp. 59–72, 2019.

[36] M. Treiber and A. Kesting, *Traffic Flow Dynamics: Data, Models and Simulation*. Springer-Verlag, Berlin, Heidelberg, 2013.

[37] W. Ren and R. W. Beard, "Consensus seeking in multiagent systems under dynamically changing interaction topologies," *IEEE Transactions on Automatic Control*, vol. 50, no. 5, pp. 655–661, 2005.

[38] S. Boyd, L. El Ghaoui, E. Feron, and V. Balakrishnan, *Linear matrix inequalities in system and control theory*. Siam, 1994, vol. 15.

[39] J. Qin and C. Yu, "Cluster consensus control of generic linear multi-agent systems under directed topology with acyclic partition," *Automatica*, vol. 49, no. 9, pp. 2898–2905, 2013.

[40] Y. Hua, X. Dong, G. Hu, Q. Li, and Z. Ren, "Distributed time-varying output formation tracking for heterogeneous linear multiagent systems with a nonautonomous leader of unknown input," *IEEE Transactions on Automatic Control*, vol. 64, no. 10, pp. 4292–4299, 2019.

[41] X. Meng and C. G. Cassandras, "A real-time optimal eco-driving approach for autonomous vehicles crossing multiple signalized intersections," in *2019 American Control Conference (ACC)*. IEEE, 2019, pp. 3593–3598.

[42] J.-J. Martinez and C. Canudas-de Wit, "A safe longitudinal control for adaptive cruise control and stop-and-go scenarios," *IEEE Transactions on control systems technology*, vol. 15, no. 2, pp. 246–258, 2007.

[43] O. Bagdadi, "Assessing safety critical braking events in naturalistic driving studies," *Transportation research part F: traffic psychology and behaviour*, vol. 16, pp. 117–126, 2013.

[44] A. Gattami, A. Al Alam, K. H. Johansson, and C. J. Tomlin, "Establishing safety for heavy duty vehicle platooning: A game theoretical approach," *IFAC Proceedings Volumes*, vol. 44, no. 1, pp. 3818–3823, 2011.

[45] V. Turri, B. Besselink, and K. H. Johansson, "Cooperative look-ahead control for fuel-efficient and safe heavy-duty vehicle platooning," *IEEE Transactions on Control Systems Technology*, vol. 25, no. 1, pp. 12–28, 2016.

[46] L. Bertoni, J. Guanetti, M. Basso, M. Masoero, S. Cetinkunt, and F. Borrelli, "An adaptive cruise control for connected energy-saving electric vehicles," *IFAC-PapersOnLine*, vol. 50, no. 1, pp. 2359–2364, 2017.

[47] B. Van Arem, C. J. Van Driel, and R. Visser, "The impact of cooperative adaptive cruise control on traffic-flow characteristics," *IEEE Transactions on intelligent transportation systems*, vol. 7, no. 4, pp. 429–436, 2006.

[48] S. E. Li, K. Deng, Y. Zheng, and H. Peng, "Effect of pulse-and-glide strategy on traffic flow for a platoon of mixed automated and manually driven vehicles," *Computer-Aided Civil and Infrastructure Engineering*, vol. 30, no. 11, pp. 892–905, 2015.

[49] M. Bando, K. Hasebe, K. Nakanishi, and A. Nakayama, "Analysis of optimal velocity model with explicit delay," *Physical Review E*, vol. 58, no. 5, p. 5429, 1998.

[50] D. Helbing and B. Tilch, "Generalized force model of traffic dynamics," *Physical review E*, vol. 58, no. 1, p. 133, 1998.

[51] P. Fernandes and U. Nunes, "Multiplatooning leaders positioning and cooperative behavior algorithms of communicant automated vehicles for high traffic capacity," *IEEE Transactions on Intelligent Transportation Systems*, vol. 16, no. 3, pp. 1172–1187, 2015.

[52] J. Hu, P. Bhowmick, F. Arvin, A. Lanzon, and B. Lennox, "Co-operative control of heterogeneous connected vehicle platoons: An adaptive leader-following approach," *IEEE Robotics and Automation Letters*, vol. 5, no. 2, pp. 977–984, 2020.

[53] Y. Zheng, S. E. Li, K. Li, and L.-Y. Wang, "Stability margin improvement of vehicular platoon considering undirected topology and asymmetric control," *IEEE Transactions on Control Systems Technology*, vol. 24, no. 4, pp. 1253–1265, 2016.

[54] Y. Zheng, S. E. Li, J. Wang, D. Cao, and K. Li, "Stability and scalability of homogeneous vehicular platoon: Study on the influence of information flow topologies," *IEEE Transactions on intelligent transportation systems*, vol. 17, no. 1, pp. 14–26, 2015.

[55] Z. Meng, B. D. Anderson, and S. Hirche, "Formation control with mismatched compasses," *Systems & Control Letters*, vol. 69, pp. 232–241, 2016.

[56] G. Wen, Z. Duan, G. Chen, and W. Yu, "Consensus tracking of multi-agent systems with lipschitz-type node dynamics and switching topologies," *IEEE Transactions on Circuits and Systems I: Regular Papers*, vol. 61, no. 2, pp. 499–511, 2014.

[57] L. Zhang, J. Wang, and C. Li, "Distributed model predictive control for polytopic uncertain systems subject to actuator saturation," *Journal of Process Control*, vol. 23, no. 8, pp. 1075–1089, 2013.

[58] Z. Zhang, W. Yan, and H. Li, "Distributed optimal control for linear multi-agent systems on general digraphs," *IEEE Transactions on Automatic Control*, p. inpress, 2020.

[59] J. Sun, Z. Zheng, and J. Sun, "Stability analysis methods and their applicability to car-following models in conventional and connected environments," *Transportation research part B: methodological*, vol. 109, pp. 212–237, 2018.

[60] R. Herman, E. W. Montroll, R. B. Potts, and R. W. Rothery, "Traffic dynamics: analysis of stability in car following," *Operations research*, vol. 7, no. 1, pp. 86–106, 1959.

[61] H. Li, Z. Gong, W. Lin, and T. Lippa, "Motion profile planning for reduced jerk and vibration residuals," *SIMTech technical reports*, vol. 8, no. 1, pp. 32–37, 2007.

[62] A. Bisoffi, F. Biral, M. Da Lio, and L. Zaccarian, "Longitudinal jerk estimation for identification of driver intention," in *2015 IEEE 18th International Conference on Intelligent Transportation Systems*. IEEE, 2015, pp. 1855–1861.

[63] F. Feng, S. Bao, J. R. Sayer, C. Flannagan, M. Manser, and R. Wunderlich, "Can vehicle longitudinal jerk be used to identify aggressive drivers? an examination using naturalistic driving data," *Accident Analysis & Prevention*, vol. 104, pp. 125–136, 2017.

[64] O. Bagdadi and A. Várhelyi, "Development of a method for detecting jerks in safety critical events," *Accident Analysis & Prevention*, vol. 50, pp. 83–91, 2013.

[65] S. K. Sharma and S. Chaturvedi, "Jerk analysis in rail vehicle dynamics," *Perspectives in Science*, vol. 8, pp. 648–650, 2016.

[66] Y. Fang, J. Hu, W. Liu, Q. Shao, J. Qi, and Y. Peng, "Smooth and time-optimal s-curve trajectory planning for automated robots and machines," *Mechanism and Machine Theory*, vol. 137, pp. 127–153, 2019.

[67] R. G. Cofield and R. Gupta, "Reactive trajectory planning and tracking for pedestrian-aware autonomous driving in urban environments," in *2016 IEEE Intelligent Vehicles Symposium (IV)*. IEEE, 2016, pp. 747–754.

[68] S. Perri, C. G. L. Bianco, and M. Locatelli, "Jerk bounded velocity planner for the online management of autonomous vehicles," in *2015 IEEE international conference on automation science and engineering (CASE)*. IEEE, 2015, pp. 618–625.

[69] A. Y. Lee and Y. Choi, "Smooth trajectory planning methods using physical limits," *Proceedings of the Institution of Mechanical Engineers, Part C: Journal of Mechanical Engineering Science*, vol. 229, no. 12, pp. 2127–2143, 2015.